with the p38 MAPK inhibitor SB203580 dramatically downregulated the expression levels of *BMP2* and *FGF2* to control levels (Figure 4C and D). In contrast, the Erk1/2 MAPK inhibitor U0126 had no effect on *FGF2* expression levels and led to a slight increase in *BMP2* expression (Figure 4C and D).

MKK6-mediated activation of p38 MAPK increases BMP2 and FGF2 expression in hADMPCs

To further confirm the involvement of p38 MAPK in the regulation of BMP2 and FGF2, hADMPCs were transduced with a lentiviral vector expressing constitutively active MKK6 (MKK6 (glu)) [30] from an EF1α promoter. As shown in Figure 5A, lentiviral transduction of MKK6 (glu) led to expression of Flag-tagged MKK6 (glu) in hADMPCs. Moreover, the expression of MKK6 (glu) resulted in activation of p38 MAPK as expected [30] (Figure 5A), and upregulation of BMP2 and FGF2 expression (Figure 5B-E).

NF-κB is not activated in hADMPCs exposed to oxidative stress

It has been reported that NF-κB directly binds to the *BMP2* promoter to induce its expression [31], and MSK1, a downstream molecule of p38 MAPK, is involved in NF-κB transactivation [32]. Therefore, we

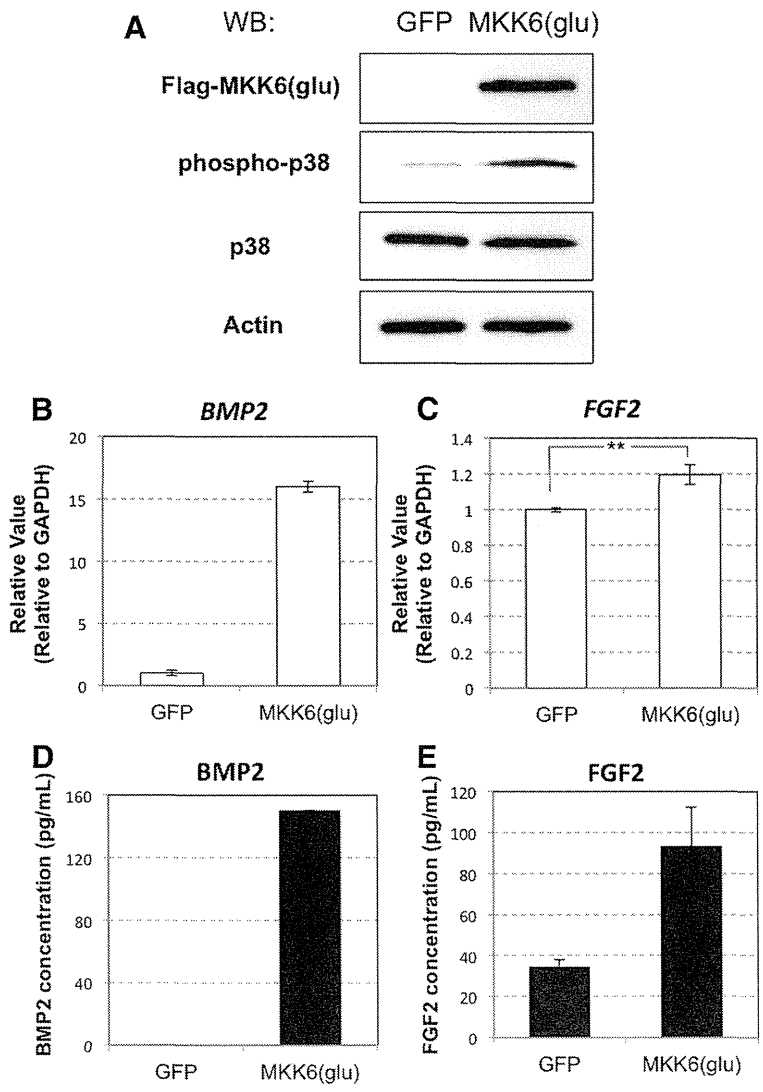

Figure 5 Activation of p38 MAPK by a constitutively active form of MKK6 resulted in elevated expression of BMP2 and FGF2. (A) A lentiviral vector expressing Flag-tagged MKK6 (glu) was transfected into hADMPCs. Expression of Flag-tagged MKK6 (glu), phosphorylated p38 MAPK and p38 MAPK was analyzed by western blotting. A CSII-EF-EGFP lentiviral vector was infected as a control (GFP). Actin was detected as an internal control. **(B, C)** Transcriptional levels of *BMP2* (**B**) and *FGF2* (**C**) were analyzed by q-PCR. The most reliable internal control gene was determined using the geNorm Software. **(D, E)** BMP2 (**D**) and FGF2 (**E**) secretion was analyzed by ELISA.

hypothesized that p38 MAPK-mediated activation of NF-κB might contribute to elevated expression of *BMP2* mRNA. To confirm this hypothesis, transcriptional activation of NF-κB was examined by measuring luciferase activity driven by the synthetic NF-κB response element. We found that transcriptional activity of NF-κB was not stimulated by BSO treatment (Figure 6A), and immunocytochemical analysis also revealed that NF-κB was not activated (nuclear localization of NF-κB/p65 was rarely observed) in BSO-treated hADMPCs (Figure 6B). These results suggested that elevated expression of *BMP2* mRNA is not mediated by NF-κB signaling.

Our current data thus demonstrate the crucial role of ROS, via activation of the p38 MAPK signaling pathway, in regulating expression levels of the neurotrophic factors BMP2 and FGF2 in hADMPCs. The overall model that we propose, based upon our findings, is shown in Figure 7.

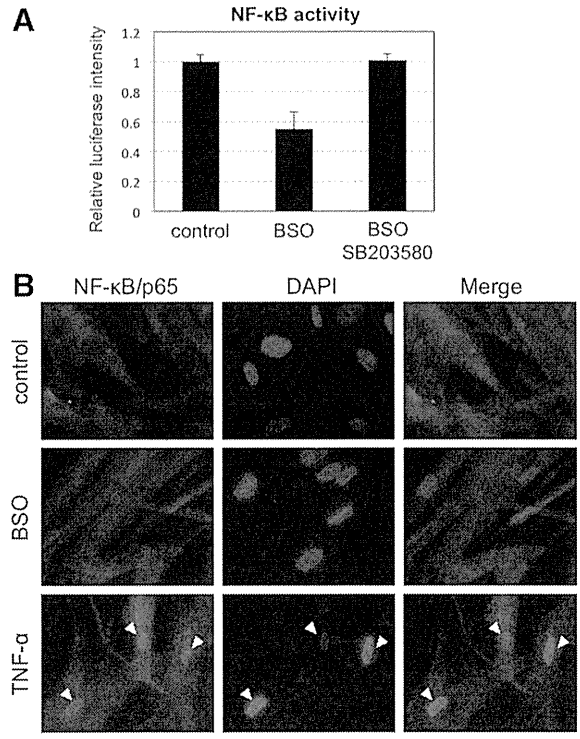

Figure 6 Transcriptional activity of NF-κB was not stimulated by oxidative stress. hADMPCs were transfected with pNF-κB-Luc and were treated with 10 μM of SB203580 or 0.1% DMSO for 2 h followed by addition of 1 mM of BSO. After 24 h, the medium was changed to fresh medium and cells were cultured for an additional 2 days. **(A)** The activity of NF-κB was measured by the intensity of luciferase activity driven from a minimal promoter containing tandem repeats of the NFκB transcriptional response element. Data shown represent the average of 3 independent experiments. **(B)** Immunocytochemical analysis against NF-κB/p65 (green). Blue staining represents nuclear staining by DAPI. Note that nuclear localization of NF-κB/p65 (white arrowhead) is only observed in hADMPCs treated with 20 ng/mL of TNF-α.

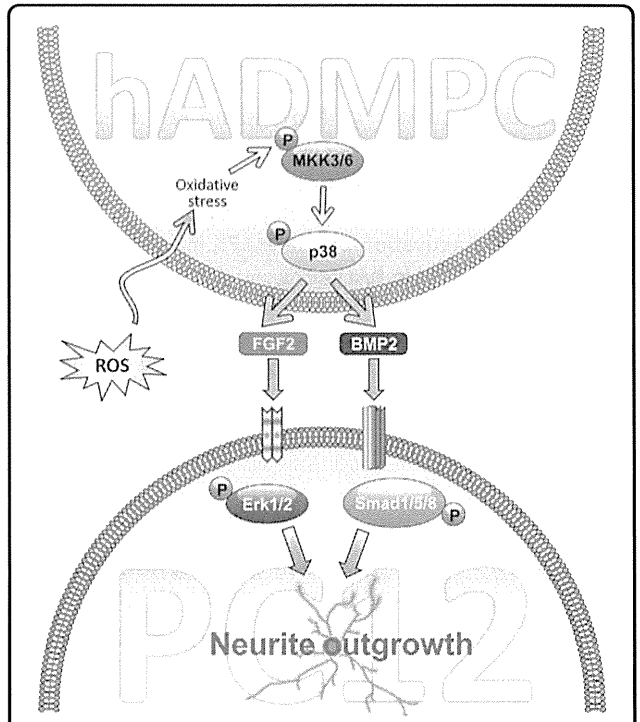

Figure 7 Model of this study. A schematic illustration of the results of this study is shown. Oxidative stress by BSO treatment in hADMPCs results in p38 MAPK activation, which then leads to BMP2 and FGF2 expression and secretion. The secreted factors then bind to the receptors on PC12 cells, facilitating neural differentiation in these cells.

Discussion

In this study, we investigated the effect of oxidative stress in hADMPCs on the induction of neuronal differentiation. Such mechanisms may explain how administration of hADMPCs to neurodegenerative lesions enhances endogenous repair mechanisms via neurogenesis of endogenous neural progenitor and stem cells. Damaged tissues, such as the brain tissue of patients who have suffered from ischemic stroke, are subject to inflammation and the generation of reactive oxygen species (ROS) [17,18]. Our data demonstrated that hADMPCs, when exposed to oxidative stress, facilitate neuronal differentiation in rat pheochromocytoma cell line PC12 cells by upregulation of fibroblast growth factor 2 (FGF2) and bone morphogenetic protein 2 (BMP2) secretion through p38 MAPK activation.

Our results show that BMP2 and FGF2 were upregulated in hADMPCs when exposed to buthionine sulfoximine (BSO), a glutathione-synthesis inhibitor that leads to oxidative stress. These findings may have therapeutic implications in neurodegenerative diseases. We concluded that BMP2 and FGF2 secreted from hADMPCs that had been exposed to oxidative stress were the main inducers of neurite outgrowth in PC12 cells. Erk1/2 and

Smad1/5/8 were significantly activated in these cells (Figure 2), while other growth factors known to induce neurite outgrowth in PC12 cells such as nerve growth factor (NGF) and vascular endothelial growth factor (VEGF) were not observed to be upregulated by BSO treatment (data not shown). We confirmed that BMP2 enhanced the effect that FGF2 had on the differentiation of PC12 cells (Figure 3), supporting our idea that hADMPCs under oxidative stress conditions secrete BMP2 and FGF2 and that this contributes to neuronal differentiation. Consistent with our conclusions, it has been reported that BMP2, via activation of a Smad signaling pathway, facilitated FGF2-induced neuronal differentiation in PC12 cells [26,27]. However, since hADMPCs have been reported to secrete many growth factor including NGF, VEGF, HGF, and IGF [11,15,33], we cannot exclude the possibility that BMP2 and FGF2 are acting cooperatively with these growth factors to facilitate neurite outgrowth in PC12 cells. Thus, the precise molecular mechanisms of induction of PC12 differentiation and the precise expression profiles in BSO-treated hADMPCs need to be further investigated.

Recently, BMP signaling through Smad1/5/8 has been reported to contribute to neurite outgrowth in dorsal root ganglion neurons both in vitro and in vivo [34,35]. Moreover, BMP2 has been shown to have neurotrophic effects on midbrain dopaminergic neurons [36], ventral mesencephalic neurons [37], mouse embryonic striatal neurons [38], and nitrergic and catecholaminergic enteric neurons [39]. Moreover, FGF2 is trophic for neurons, glias, and endothelial cells in the central nervous system. FGF2 also prevents downregulation of the anti-apoptotic protein Bcl-2 in ischemic brain tissue and limits excitotoxic damage to the brain through an activin-dependent mechanism [40]. These findings are consistent with our hypothesis that hADMPCs secret BMP2 and FGF2 to induce neurogenesis in neurodegenerative lesions in response to oxidative stress.

As it has been shown that ROS activate ERKs, JNKs, and p38 MAPKs [28,29], we examined the MAPK signaling pathway in hADMPCs exposed to oxidative stress and found that BSO treatment resulted in significant activation of ERK1/2 and p38 MAPK. Intriguingly, addition of SB203580, a specific inhibitor of p38 MAPK, but not the ERK inhibitor U0126, suppressed *BMP2* and *FGF2* expression in BSO-treated hADMPCs to control levels (Figure 4), suggesting that p38 MAPK was contributing to upregulation of BMP2 and FGF2 in hADMPCs when exposed to oxidative stress. Moreover, lentiviral transduction of the constitutively active form of MKK6, a MAPKK that selectively activates p38 MAPK isoforms [30], resulted in upregulation of BMP2 and FGF2 and this also demonstrated the crucial role of the p38 MAPK cascade in the regulation of BMP2 and FGF2. In primary human endothelial cells, p38-dependent regulation of BMP2 expression was reported previously. Viemann *et al.* [41] investigated the genes that were induced by inflammatory stimulation with tumor necrosis factor α (TNF-α) and classified these genes into 2 categories based on whether they were regulated in an NF-κB-dependent or p38 MAPK-dependent manner. Consistent with our findings, they found that significant induction of BMP2 expression by TNF-α was markedly suppressed by SB202190, an inhibitor of p38 MAPK. These results support the hypothesis that activation of the p38 MAPK pathway in hADMPCs in response to inflammation surrounding neurodegenerative lesions leads to induction of BMP2 and FGF2, which in turn support regeneration of neuronal cells.

It has been known that NF-κB directly binds to the BMP2 promoter to induce its expression [31], and MSK1, a downstream molecule of p38 MAPK, is involved in NF-κB transactivation [32]. However, we did not observe an elevation of NF-κB transcriptional activity in hADMPCs when they were exposed to oxidative stress (Figure 6). The mechanism of p38-dependent regulation of gene expression is not completely understood, and the precise mechanism by which p38 MAPK regulates the expression of BMP2 and FGF2 remains to be determined.

In this study, we also found that suppression of ERK1/2 MAPK by U0126 in BSO-treated hADMPCs resulted in slight activation of p38 MAPK (Figure 4A). Consistent with this, the expression level of *BMP2* mRNA was also upregulated when cells exposed to oxidative stress were pretreated with U0126 (Figure 4C). Previously, "seesaw cross-talk" between ERK and p38 MAPK signaling has been reported; i.e., the MEK inhibitor caused a decrease in the phosphorylation level of ERK and an increase in that of p38, whereas the p38 inhibitor had the opposite effect [42-44]. We did not investigate the phosphorylation of ERK1/2 in SB203580-treated hADMPCs, but it may be possible that seesaw cross-talk also occurs in our system.

Conclusions

In summary, the results obtained in this study have demonstrated the potential use of hADMPCs for the treatment of neurodegenerative diseases such as ischemic stroke, Parkinson's disease, Alzheimer's disease, and spinal cord injury, in which the transplanted hADMPCs might be exposed to oxidative stress. Moreover, the p38-dependent modulation of BMP2 and FGF2 expression observed in this study is expected to be a new therapeutic target for neurodegenerative disorders.

Materials and methods

Adipose tissue samples

Subcutaneous adipose tissue samples (10–50 g, each) were resected during plastic surgery in 5 females (age,

20–60 years) as excess discards. The study protocol was approved by the Review Board for Human Research of Kobe University Graduate School of Medicine, Foundation for Biomedical Research and Innovation and Kinki University Pharmaceutical Research and Technology Institute (reference number: 10–005). Each subject provided a signed informed consent.

Cell culture

PC12 cells were obtained from the Health Science Research Resources Bank (Osaka, Japan) and maintained in RPMI1640 media supplemented with 10% heat-inactivated horse serum and 5% fetal bovine serum. For differentiation, the cells were plated in 6-well culture plates coated with collagen type I (Nitta Gelatin, Osaka, Japan) and the medium was replaced with differentiation medium (RPMI1640 supplemented with 1% horse serum and 0.5% fetal bovine serum) or conditioned medium from hADMPCs. NGF (50 ng/mL), BMP2 (40 ng/mL) or FGF2 (5 ng/mL) were added to the differentiation medium. Recombinant murine Noggin (200 ng/mL: PeproTech, NJ, USA) was added to conditioned medium from BSO-treated hADMPCs. hADMPCs were isolated as previously reported [4-6,45,46] and maintained in a medium containing 60% DMEM-low glucose, 40% MCDB-201 medium (Sigma Aldrich, St. Louis, MO, USA), 1× insulin-transferrin-selenium (Gibco Invitrogen, NY, USA), 1 nM dexamethasone (Sigma Aldrich), 100 mM ascorbic acid 2-phosphate (Wako, Osaka, Japan), 10 ng/mL epidermal growth factor (PeproTech), and 5% fetal bovine serum. The cells were plated to a density of 5×10^3 cells/cm^2 on fibronectin-coated dishes, and the medium was replaced every 2 days.

Preparation of conditioned medium from hADMPCs

Two days after plating, hADMPCs were treated with BSO (concentrations used were varied in each experiment and are indicated in the results and figure legends) for 16 h. The medium was replaced with fresh culture medium for 2 days followed by replacement with PC12 cell differentiation medium. After 2 more days, the medium was removed for use as conditioned medium. For preparation of the conditioned medium from hADMPCs in which one of the three, p38, Erk1/2, or JNK MAPK, was inhibited, hADMPCs were pretreated with 10 μM SB203580 (Promega, WI, USA), 10 μM U0126 (Promega), or 10 μM JNK inhibitor II (EMD4 Bioscience, CA, USA), respectively, for 2 h and subsequently treated with 1 mM BSO.

Measurement of GSH/GSSG ratio

Ratios of reduced glutathione (GSH) to oxidized glutathione (GSSG) were measured using the GSH/GSSG-Glo assay kit (Promega) following the manufacturer's protocol.

Measurement of reactive oxygen species production

Cells were harvested and incubated with 10 μM 5-(and-6)-chloromethyl-2′,7′-dichlorodihydrofluorescein diacetate, acetyl ester (CM-H_2DCFDA). The amount of intracellular ROS production was proportional to green fluorescence, as analyzed with a Guava easyCyte 8HT flow cytometer (Millipore) using an argon laser at 488 nm and a 525/30 nm band pass filter, and dead cells were excluded with the LIVE/DEAD fixable far red dead cell stain kit (Invitrogen).

Western blot analysis

Cells were washed with ice-cold phosphate-buffered saline and lysed with M-PER Mammalian Protein Extraction Reagent (Thermo Scientific Pierce, IL, USA) following the manufacturer's instructions. Equal amounts of proteins were separated by sodium dodecylsulfate polyacrylamide gel electrophoresis (SDS-PAGE), transferred to polyvinylidene fluoride (PVDF) membranes (Immobilon-P; Millipore, MA, USA), and probed with antibodies against phospho-Erk1/2 (#4370), Erk1/2 (#4695), phospho-38 (#9215), p38 (#9212), phospho-Smad1/5/8 (#9511), phospho-Akt (#4060), Akt (#4691), phospho-JNK (#9251), JNK (#9258) (all from Cell Signaling Technology, MA, USA) and actin (Millipore). Horseradish peroxidase (HRP)-conjugated anti-rabbit and anti-mouse secondary antibodies (Cell Signaling Technology, Danvers, MA, USA) were used as probes and immunoreactive bands were visualized with the Immobilon Western Chemiluminescent HRP substrate (Millipore). The band intensity was measured using ImageJ software.

RNA extraction, cDNA generation, and quantitative polymerase chain reaction (q-PCR)

Total RNA was extracted using the RNeasy Mini Kit (Qiagen, Hilden, Germany) following the manufacturer's instructions. cDNA was generated from 1 μg of total RNA using the Verso cDNA Synthesis Kit (Thermo Scientific) and purified with the MinElute PCR Purification Kit (Qiagen). Q-PCR analysis was carried out using the SsoFast EvaGreen supermix (Bio-Rad, CA, USA) according to the manufacturer's protocols. The relative expression value of each gene was calculated using a ΔΔCt method and the most reliable internal control gene was determined using the geNorm Software (http://medgen.ugent.be/~jvdesomp/genorm/). Details of the primers used in these experiments are available on request.

Enzyme-linked immunosorbent assay

Enzyme-linked immunosorbent assay (ELISA) was performed using the Quantikine BMP-2 Immunoassay System and Quantikine FGF-2 Immunoassay System (R&D

Systems, MN, USA) following the manufacturer's protocols.

Plasmid construction and lentivirus production

Flag-tagged MKK6 (glu) [30] was provided by Addgene (pcDNA3-Flag MKK6 (glu); Addgene plasmid 13518). Flag-tagged MKK6 (glu) was cloned into a pENTR11 vector (Invitrogen). An iresGFP fragment was subsequently cloned into the plasmid to produce the entry vector pENTR11-MKK6 (glu)-iresGFP. The entry vector and CSII-EF-RfA (kindly provided by Dr. Miyoshi, RIKEN BioResource Center, Tsukuba, Japan) were incubated with LR clonase II enzyme mix (Invitrogen) to generate CSII-EF-MKK6 (glu)-iresGFP. The resultant plasmid was mixed with packaging plasmids (pCAG-HIVg/p and pCMV-VSVG-RSV-Rev, kindly provided by Dr. Miyoshi) and transfected into 293 T cells. The supernatant medium, which contained lentiviral vectors, was collected 2 days after transduction and concentrated by centrifugation (6000 G, 15 h, 4°C).

Luciferase assay

hADMPCs were transfected with pGL4.74 (Promega) and either pTAL-Luc or pNF-κB-Luc by TransIT-2020 (TaKaRa-Bio). The cells were then treated with 10 μM of SB203580 or 0.1% DMSO for 2 h followed by addition of 1 mM of BSO. After 24 h, the medium was changed to fresh medium and cells were cultured for an additional 2 days. The activity of NF-κB was measured using the Dual Luciferases Assay System (Promega) according to the manufacturer's protocol.

Immunocytochemistry

hADMPCs were fixed with 4% paraformaldehyde in PBS for 10 min at 4°C and then washed 3 times in PBS. Blocking was performed with PBSMT (PBS containing 0.1% Triton X-100, 2% Skim Milk) for 1 h at room temperature. The cells were then incubated with rabbit monoclonal antibody against NF-κB p65 (Cell Signaling; #8242; 1/100 dilution) overnight at 4°C. After washing with PBS, cells were incubated with Alexa 488 conjugated anti-rabbit IgG (Invitrogen; 1/1000 dilution) for 1 h. The cells were counterstained with 4′-6-diamidino-2-phenylindole (DAPI) (Invitrogen) to identify cellular nuclei.

Competing interests

None of the authors have any competing interests related to the manuscript.

Authors' contributions

MM carried out the FACS analysis, qPCR analysis, ELISA, immunofluorescent staining, and cell culture, participated in the study design, and drafted the manuscript. HM participated in the study design, carried out the western blot analysis, luciferase assay, and cell culture, and drafted the manuscript. AU carried out western blot analysis, constructed the plasmids, and generated the lentiviral vectors. YN carried out qPCR analysis and performed the statistical analysis. AI resected subcutaneous adipose tissue samples during plastic surgery. HO and AM isolated hADMPCs from human adipose tissues. TH conceived the study, participated in its design and coordination, and helped to draft the manuscript. All authors read and approved the final manuscript.

Acknowledgements

We thank A Nishikawa, T Fukase, T Sasaki, T Shoji, K Nakagita, S Fukui, and K Honjo for technical support. We thank Dr. Roger Davis for providing the pcDNA3-Flag MKK6 (glu) plasmid and Dr. Hiroyuki Miyoshi for the CSII-EF-RfA, pCMV-VSVG-RSV-Rev and pCMV-HIVg/p plasmids. This work was supported in part by grants from the Ministry of Health, Labor, and Welfare of Japan and a grant from the Program for Promotion of Fundamental Studies in Health Sciences of the National Institute of Biomedical Innovation (NIBIO).

Author details

[1]Pharmaceutical Research and Technology Institute, Kinki University, 3-4-1 Kowakae, Higashi-Osaka, Osaka 577-8502, Japan. [2]Department of Somatic Stem Cell Therapy and Health Policy, Foundation for Biomedical Research and Innovation, TRI305, 1-5-4 Minatojima-minamimachi, Chuo-ku, Kobe, Hyogo 650-0047, Japan. [3]Department of Plastic Surgery, Kobe University Hospital, Kobe, Japan.

Received: 28 March 2012 Accepted: 2 August 2012
Published: 7 August 2012

References

1. Pittenger MF, Mackay AM, Beck SC, Jaiswal RK, Douglas R, Mosca JD, Moorman MA, Simonetti DW, Craig S, Marshak DR: **Multilineage potential of adult human mesenchymal stem cells.** *Science* 1999, **284**:143–147.
2. Bieback K, Kern S, Kluter H, Eichler H: **Critical parameters for the isolation of mesenchymal stem cells from umbilical cord blood.** *Stem Cells* 2004, **22**:625–634.
3. Zuk PA, Zhu M, Ashjian P, De Ugarte DA, Huang JI, Mizuno H, Alfonso ZC, Fraser JK, Benhaim P, Hedrick MH: **Human adipose tissue is a source of multipotent stem cells.** *Mol Biol Cell* 2002, **13**:4279–4295.
4. Okura H, Komoda H, Saga A, Kakuta-Yamamoto A, Hamada Y, Fumimoto Y, Lee CM, Ichinose A, Sawa Y, Matsuyama A: **Properties of hepatocyte-like cell clusters from human adipose tissue-derived mesenchymal stem cells.** *Tissue Eng Part C Methods* 2010, **16**:761–770.
5. Okura H, Matsuyama A, Lee CM, Saga A, Kakuta-Yamamoto A, Nagao A, Sougawa N, Sekiya N, Takekita K, Shudo Y, *et al*: **Cardiomyoblast-like cells differentiated from human adipose tissue-derived mesenchymal stem cells improve left ventricular dysfunction and survival in a rat myocardial infarction model.** *Tissue Eng Part C Methods* 2010, **16**:417–425.
6. Komoda H, Okura H, Lee CM, Sougawa N, Iwayama T, Hashikawa T, Saga A, Yamamoto-Kakuta A, Ichinose A, Murakami S, Sawa Y, Matsuyama A: **Reduction of N-glycolylneuraminic acid xenoantigen on human adipose tissue-derived stromal cells/mesenchymal stem cells leads to safer and more useful cell sources for various stem cell therapies.** *Tissue Eng Part A* 2010, **16**:1143–1155.
7. Okura H, Komoda H, Fumimoto Y, Lee CM, Nishida T, Sawa Y, Matsuyama A: **Transdifferentiation of human adipose tissue-derived stromal cells into insulin-producing clusters.** *J Artif Organs* 2009, **12**:123–130.
8. Safford KM, Safford SD, Gimble JM, Shetty AK, Rice HE: **Characterization of neuronal/glial differentiation of murine adipose-derived adult stromal cells.** *Exp Neurol* 2004, **187**:319–328.
9. Leu S, Lin YC, Yuen CM, Yen CH, Kao YH, Sun CK, Yip HK: **Adipose-derived mesenchymal stem cells markedly attenuate brain infarct size and improve neurological function in rats.** *J Transl Med* 2010, **8**:63.
10. Ikegame Y, Yamashita K, Hayashi S, Mizuno H, Tawada M, You F, Yamada K, Tanaka Y, Egashira Y, Nakashima S, Yoshimura S, Iwama T: **Comparison of mesenchymal stem cells from adipose tissue and bone marrow for ischemic stroke therapy.** *Cytotherapy* 2011, **13**:675–685.
11. Tan B, Luan Z, Wei X, He Y, Wei G, Johnstone BH, Farlow M, Du Y: **AMP-activated kinase mediates adipose stem cell-stimulated neuritogenesis of PC12 cells.** *Neuroscience* 2011, **181**:40–47.
12. Reid AJ, Sun M, Wiberg M, Downes S: *Terenghi G.* Kingham PJ: Nerve repair with adipose-derived stem cells protects dorsal root ganglia neurons from apoptosis. Neuroscience; 2011.

13. Rehman J, Traktuev D, Li J, Merfeld-Clauss S, Temm-Grove CJ, Bovenkerk JE, Pell CL, Johnstone BH, Considine RV, March KL: **Secretion of angiogenic and antiapoptotic factors by human adipose stromal cells.** *Circulation* 2004, **109**:1292–1298.
14. Lee EY, Xia Y, Kim WS, Kim MH, Kim TH, Kim KJ, Park BS, Sung JH: **Hypoxia-enhanced wound-healing function of adipose-derived stem cells: increase in stem cell proliferation and up-regulation of VEGF and bFGF.** *Wound Repair Regen* 2009, **17**:540–547.
15. Lu S, Lu C, Han Q, Li J, Du Z, Liao L, Zhao RC: **Adipose-derived mesenchymal stem cells protect PC12 cells from glutamate excitotoxicity-induced apoptosis by upregulation of XIAP through PI3-K/Akt activation.** *Toxicology* 2011, **279**:189–195.
16. McCoy MK, Martinez TN, Ruhn KA, Wrage PC, Keefer EW, Botterman BR, Tansey KE, Tansey MG: **Autologous transplants of Adipose-Derived Adult Stromal (ADAS) cells afford dopaminergic neuroprotection in a model of Parkinson's disease.** *Exp Neurol* 2008, **210**:14–29.
17. Flamm ES, Demopoulos HB, Seligman ML, Poser RG, Ransohoff J: **Free radicals in cerebral ischemia.** *Stroke* 1978, **9**:445–447.
18. Alexandrova ML, Bochev PG: **Oxidative stress during the chronic phase after stroke.** *Free Radic Biol Med* 2005, **39**:297–316.
19. Lambeth JD: **NOX enzymes and the biology of reactive oxygen.** *Nat Rev Immunol* 2004, **4**:181–189.
20. Simpson JE, Ince PG, Haynes LJ, Theaker R, Gelsthorpe C, Baxter L, Forster G, Lace GL, Shaw PJ, Matthews FE, Savva GM, Brayne C, Wharton SB, MRC Cognitive Function and Ageing Neuropathology Study Group: **Population variation in oxidative stress and astrocyte DNA damage in relation to Alzheimer-type pathology in the ageing brain.** *Neuropathol Appl Neurobiol* 2010, **36**:25–40.
21. Cai Z, Zhao B, Ratka A: **Oxidative Stress and beta-Amyloid Protein in Alzheimer's Disease.** *Neuromolecular Med* 2011, **13**:223–250.
22. Beal MF: **Mitochondria, oxidative damage, and inflammation in Parkinson's disease.** *Ann N Y Acad Sci* 2003, **991**:120–131.
23. Henchcliffe C, Beal MF: **Mitochondrial biology and oxidative stress in Parkinson disease pathogenesis.** *Nat Clin Pract Neurol* 2008, **4**:600–609.
24. Minghetti L, Ajmone-Cat MA, De Berardinis MA, De Simone R: **Microglial activation in chronic neurodegenerative diseases: roles of apoptotic neurons and chronic stimulation.** *Brain Res Brain Res Rev* 2005, **48**:251–256.
25. Colton CA, Chernyshev ON, Gilbert DL, Vitek MP: **Microglial contribution to oxidative stress in Alzheimer's disease.** *Ann N Y Acad Sci* 2000, **899**:292–307.
26. Hayashi H, Ishisaki A, Suzuki M, Imamura T: **BMP-2 augments FGF-induced differentiation of PC12 cells through upregulation of FGF receptor-1 expression.** *J Cell Sci* 2001, **114**:1387–1395.
27. Hayashi H, Ishisaki A, Imamura T: **Smad mediates BMP-2-induced upregulation of FGF-evoked PC12 cell differentiation.** *FEBS Lett* 2003, **536**:30–34.
28. Son Y, Cheong YK, Kim NH, Chung HT, Kang DG, Pae HO: **Mitogen-Activated Protein Kinases and Reactive Oxygen Species: How Can ROS Activate MAPK Pathways?** *J Signal Transduct* 2011, **2011**:792639.
29. Ito K, Hirao A, Arai F, Takubo K, Matsuoka S, Miyamoto K, Ohmura M, Naka K, Hosokawa K, Ikeda Y, Suda T: **Reactive oxygen species act through p38 MAPK to limit the lifespan of hematopoietic stem cells.** *Nat Med* 2006, **12**:446–451.
30. Raingeaud J, Whitmarsh AJ, Barrett T, Derijard B, Davis RJ: **MKK3- and MKK6-regulated gene expression is mediated by the p38 mitogen-activated protein kinase signal transduction pathway.** *Mol Cell Biol* 1996, **16**:1247–1255.
31. Feng JQ, Xing L, Zhang JH, Zhao M, Horn D, Chan J, Boyce BF, Harris SE, Mundy GR, Chen D: **NF-kappaB specifically activates BMP-2 gene expression in growth plate chondrocytes in vivo and in a chondrocyte cell line in vitro.** *J Biol Chem* 2003, **278**:29130–29135.
32. Vermeulen L, De Wilde G, Van Damme P: **Vanden Berghe W, Haegeman G: Transcriptional activation of the NF-kappaB p65 subunit by mitogen- and stress-activated protein kinase-1 (MSK1).** *EMBO J* 2003, **22**:1313–1324.
33. Rasmussen JG, Frobert O, Pilgaard L, Kastrup J, Simonsen U, Zachar V, Fink T: **Prolonged hypoxic culture and trypsinization increase the pro-angiogenic potential of human adipose tissue-derived stem cells.** *Cytotherapy* 2011, **13**:318–328.
34. Parikh P, Hao Y, Hosseinkhani M, Patil SB, Huntley GW, Tessier-Lavigne M, Zou H: **Regeneration of axons in injured spinal cord by activation of bone morphogenetic protein/Smad1 signaling pathway in adult neurons.** *Proc Natl Acad Sci U S A* 2011, **108**:E99–E107.
35. Ma CH, Brenner GJ, Omura T, Samad OA, Costigan M, Inquimbert P, Niederkofler V, Salie R, Sun CC, Lin HY, Arber S, Coppola G, Woolf CJ, Samad TA: **The BMP coreceptor RGMb promotes while the endogenous BMP antagonist noggin reduces neurite outgrowth and peripheral nerve regeneration by modulating BMP signaling.** *J Neurosci* 2011, **31**:18391–18400.
36. Jordan J, Bottner M, Schluesener HJ, Unsicker K, Krieglstein K: **Bone morphogenetic proteins: neurotrophic roles for midbrain dopaminergic neurons and implications of astroglial cells.** *Eur J Neurosci* 1997, **9**:1699–1709.
37. Reiriz J, Espejo M, Ventura F, Ambrosio S, Alberch J: **Bone morphogenetic protein-2 promotes dissociated effects on the number and differentiation of cultured ventral mesencephalic dopaminergic neurons.** *J Neurobiol* 1999, **38**:161–170.
38. Stull ND, Jung JW, Iacovitti L: **Induction of a dopaminergic phenotype in cultured striatal neurons by bone morphogenetic proteins.** *Brain Res Dev Brain Res* 2001, **130**:91–98.
39. Anitha M, Shahnavaz N, Qayed E, Joseph I, Gossrau G, Mwangi S, Sitaraman SV, Greene JG, Srinivasan S: **BMP2 promotes differentiation of nitrergic and catecholaminergic enteric neurons through a Smad1-dependent pathway.** *Am J Physiol Gastrointest Liver Physiol* 2010, **298**:G375–G383.
40. Ikeda N, Nonoguchi N, Zhao MZ, Watanabe T, Kajimoto Y, Furutama D, Kimura F, Dezawa M, Coffin RS, Otsuki Y, Kuroiwa T, Miyatake S: **Bone marrow stromal cells that enhanced fibroblast growth factor-2 secretion by herpes simplex virus vector improve neurological outcome after transient focal cerebral ischemia in rats.** *Stroke* 2005, **36**:2725–2730.
41. Viemann D, Goebeler M, Schmid S, Klimmek K, Sorg C, Ludwig S, Roth J: **Transcriptional profiling of IKK2/NF-kappa B- and p38 MAP kinase-dependent gene expression in TNF-alpha-stimulated primary human endothelial cells.** *Blood* 2004, **103**:3365–3373.
42. Hotokezaka H, Sakai E, Kanaoka K, Saito K, Matsuo K, Kitaura H, Yoshida N, Nakayama K: **U0126 and PD98059, specific inhibitors of MEK, accelerate differentiation of RAW264.7 cells into osteoclast-like cells.** *J Biol Chem* 2002, **277**:47366–47372.
43. Shimo T, Matsumura S, Ibaragi S, Isowa S, Kishimoto K, Mese H, Nishiyama A, Sasaki A: **Specific inhibitor of MEK-mediated cross-talk between ERK and p38 MAPK during differentiation of human osteosarcoma cells.** *J Cell Commun Signal* 2007, **1**:103–111.
44. Al-Shanti N, Stewart CE: **PD98059 enhances C2 myoblast differentiation through p38 MAPK activation: a novel role for PD98059.** *J Endocrinol* 2008, **198**:243–252.
45. Okura H, Saga A, Fumimoto Y, Soeda M, Moriyama M, Moriyama H, Nagai K, Lee CM, Yamashita S, Ichinose A, Hayakawa T, Matsuyama A: **Transplantation of human adipose tissue-derived multilineage progenitor cells reduces serum cholesterol in hyperlipidemic Watanabe rabbits.** *Tissue Eng Part C Methods* 2011, **17**:145–154.
46. Saga A, Okura H, Soeda M, Tani J, Fumimoto Y, Komoda H, Moriyama M, Moriyama H, Yamashita S, Ichinose A, Daimon T, Hayakawa T, Matsuyama A: **HMG-CoA reductase inhibitor augments the serum total cholesterol-lowering effect of human adipose tissue-derived multilineage progenitor cells in hyperlipidemic homozygous Watanabe rabbits.** *Biochem Biophys Res Commun* 2011, **412**:50–54.

doi:10.1186/1471-2121-13-21
Cite this article as: Moriyama *et al.*: Human adipose tissue-derived multilineage progenitor cells exposed to oxidative stress induce neurite outgrowth in PC12 cells through p38 MAPK signaling. *BMC Cell Biology* 2012 **13**:21.

Adipose Tissue-Derived Multi-lineage Progenitor Cells as a Promising Tool for *In Situ* Stem Cell Therapy

Hanayuki Okura[1], Ayami Saga[1], Mayumi Soeda[1], Akihiro Ichinose[2] and Akifumi Matsuyama[1,3,*]

[1]*Department of Somatic Stem Cell Therapy and Health Policy, Foundation for Biomedical Research and Innovation, 2-2 Minatojima-minamimachi, Chuo-ku, Kobe, 650-0047, Japan*

[2]*Department of Plastic Surgery, Kobe University Hospital, 7-5-2 Kusunoki-cho, Chuo-ku, Kobe, Hyogo, 650-0017, Japan*

[3]*The Center for Medical Engineering and Informatics, Osaka University, 2-2 Yamada-oka, Suita, Osaka, 565-0871, Japan*

Abstract: Adipose tissue-derived cell sources are attractive for regenerative medicine due to the easy and safe accessibility of adipose tissue, lack of ethical issues, and their availability in large quantities. We have developed an isolation method for distinct stem cells, and named the cells adipose tissue-derived multilineage progenitor cells (ADMPC). ADMPC have higher potential for differentiation into adipocytic, osteocytic, and chondrocytic progeny than the widely reported adipose tissue-derived stromal/stem cells (ADSC). ADMPC can also differentiate into hepatocyte-like clusters *in vitro* by induction with the hepatogenic cytokines, hepatocyte growth factor, oncostatin M, and basic fibroblast growth factor. *In vivo*, ADMPC were reprogrammed *in situ* into hepatocyte-like cells that corrected the metabolic defect in hyperlipidemic Watanabe rabbits after transplantation *via* the portal vein. Such cells are potentially useful in regenerative medicine as sources for *in situ* stem cell therapy.

Keywords: adipose tissue, ADMPC, *in situ* stem cell therapy, *in situ* reprogramming, *in situ* differentiation, ADSC, ADMSC, ASC.

1. INTRODUCTION

The recent finding of differentiation-capable adult somatic stem cells holds great promise for regenerative medicine [1]. Extensive research is also ongoing into mesenchymal stem cells (MSC), found in human bone marrow, scalp tissue, placenta, umbilical cord matrix, and various fetal tissues [2-6]. Among these MSC sources, adipose tissue is particularly attractive for regenerative medicine because the tissues can be easily and safely accessed, are free of any ethical issues, and are available in large amounts. Many investigators have also reported that the cells derived from adipose tissue (adipose tissue-derived stromal/stem cells [ADSC], also referred to as adipose tissue-derived mesenchymal stem cells [ADMSC]) could differentiate into various cell types *in vitro* including chondrocytes, osteoblasts, adipocytes, myocytes, neuronal cells, and hepatocytes [1-4]. ADSC are considered as a colony-forming cell-rich fraction of adherent cells, which can attach to plastic culture dishes after isolation of the stromal vascular fraction (SVF), and thereafter be expanded and maintained in monolayer cultures as a heterogeneous population [7]. However, although ADSC can differentiate into various cell types *in vitro*, their self-renewal potency decreases significantly with passaging making them unsuitable for regenerative medicine applications.

*Address correspondence to this author at the Department of Somatic Stem Cell Therapy and Health Policy, Foundation for Biomedical Research and Innovation, 2-2 Minatojima-minamimachi, Chuo-ku, Kobe, 650-0047, Japan; Tel: +81-78-304-8706; Fax: +81-78-304-8707;
E-mail: akifumi-matsuyama@umin.ac.jp

In this review, we describe a novel population of adipose tissue-derived stem cells with higher differentiation potential than other well-reported adipose tissue-derived cells; we named these adipose tissue-derived multi-lineage progenitor cells (ADMPC). ADMPC could differentiate into hepatocyte-like cells *in vitro*, and in the hepatic environment *in vivo*. These *in situ* reprogrammed cells successfully corrected the metabolic defect in diseased animals, indicating that such *in situ* reprogramming could be applied for regenerative medicine as "*in situ* stem cell therapy".

2. MATERIALS AND METHODS

2.1. Adipose Tissues

Adipose tissues were resected from five human subjects as excess discards during plastic surgery (females, age, 20-60 years). Ten to fifty grams of subcutaneous adipose tissue were collected from each subject. All subjects provided informed consent and the Review Board for Human Research of Kobe University Graduate School of Medicine and Foundation for Biomedical Research and Innovation approved the study protocol.

2.2. Isolation of ADMPC

Human ADMPC (hADMPC) were prepared as described previously [8-13]. Briefly, the resected adipose tissue was minced and then digested at 37°C for 1 h in Hank's balanced salt solution (HBSS, GIBCO Invitrogen, Grand Island, NY) containing 0.075% collagenase type II (Sigma Aldrich, St. Louis, MO). Digests were filtered through a cell strainer (BD Bioscience, San Jose, CA) and centrifuged at 800 x *g* for 10

2211-5439/12 $58.00+.00

min. Red blood cells were excluded using density gradient centrifugation with Lymphoprep (d = 1.077; Nacalai Tesque, Kyoto, Japan), and the remaining cells were cultured in Dulbecco's modified Eagle's medium (DMEM, GIBCO Invitrogen) with 10% defined fetal bovine serum (FBS, GIBCO Invitrogen) for 24 h at 37°C. Following incubation, the adherent cells were washed extensively and then treated with 0.2 g/l ethylenediaminetetraacetate (EDTA) solution (Nacalai Tesque). The resulting suspended cells were replated at a density of 10,000 cells/cm^2 on human fibronectin (FN)-coated dishes (AGC, Tokyo, Japan) in Stem Cell Medium (Nipro, Osaka, Japan) containing 1 x insulin-transferrin selenium (ITS, GIBCO Invitrogen.), 1 nM dexamethasone (Sigma Aldrich), 100 μM ascorbic acid 2-phosphate (Sigma Aldrich), 10 ng/ml epidermal growth factor (EGF, PeproTec, Rocky Hill, NJ), and 5% FBS. After passaging 5 to 6 times in the same medium, the ADMPC were ready for use in experiments. ADSC were isolated and cultured as reported by Zuk *et al.* [7].

2.3. Adipocytic, Osteocytic, and Chondrocytic Differentiation Procedure

For adipocytic differentiation, cells were cultured in Differentiation Medium (Zen-Bio, Research Triangle Park, NC) [14]. After three days, half of the medium was replaced with Adipocyte Medium (Zen-Bio) and this was repeated every two days. Five days after differentiation, adipocytes were identified by intracellular lipid droplets observed microscopically after Oil Red O staining. In brief, cultures were fixed in Baker's formal calcium, washed in 60% isopropanol, and stained with double-filtered Oil Red O solution to identify lipid accumulation. To determine the lipid content, Oil-Red O was extracted from the differentiated cells with isopropanol and absorbance of the contents was evaluated. Osteocytic differentiation was induced by culturing the cells in DMEM containing 10 nM dexamethasone, 50 mg/dl ascorbic acid 2-phosphate, 10 mM beta-glycerophosphate (Sigma Aldrich), and 10% FBS. Differentiation was evaluated by Alizarin red staining and alkaline phosphatase (ALPase) activity as described previously [15]. For Alizarin red staining, the cells were washed three times and fixed with dehydrated ethanol. After fixation, the cells were stained with 1% Alizarin red S in 0.1% NH_4OH (ph 6.5) for 5 minutes, and then washed with H_2O. ALPase activity per cell was calculated based on the amount of DNA. For chondrocytic differentiation, ADMPC were trypsinized and 2 x 10^5 cells were centrifuged at 400 x *g* for 10 minutes. The resulting pellets were cultured in chondrogenic medium (α-MEM supplemented with 10 ng/ml transforming growth factor (TGF)-β, 10 nM dexamethasone, 100 μM ascorbate, and 10 μl/ml 100 x ITS Solution) for 14 days [8]. The osteogenic differentiation was assessed by Alcian Blue staining, whereby nuclear counterstaining with Weigert's hematoxylin was followed by 0.5% Alcian Blue 8GX, which binds proteoglycan-rich cartilage matrix.

2.4. Differentiation of Hepatocyte-Like Cell Clusters

The differentiation procedure consisted of three stages. In stage I, ADMSC were cultured and expanded in medium I for three to four passages. In stage II, the cells were dissociated with trypsin-EDTA and the resulting single cells were suspended in medium II (80% knockout-DMEM [GIBCO Invitrogen], 20% defined FBS, 1 mM glutamine, and 1% nonessential amino acids [both from GIBCO Invitrogen]). The suspension was placed in an ultralow-attachment culture dish (Hydrocell; CellSeed, Tokyo, Japan), and the cells self-aggregated into cell clusters within 1 day. The cell clusters were then cultured for an additional 2 days. In stage III, after washing extensively with PBS, 2-day-old cell clusters (average of 1000 cells each) were cultured on a Hydrocell dish for 4 weeks in medium III (60% DMEM-low glucose, 40% MCDB-201, 1 nM dexamethasone, 100 mM ascorbic acid, 10 ng/ml EGF, basic fibroblast growth factor [bFGF, Peprotech, Rocky Hill, NJ], hepatocyte growth factor [HGF, Peprotech], and oncostatin M [OSM]). Finally, 0.1% dimethyl sulfoxide (DMSO; Nacalai Tesque) was added on the 10th day after induction of differentiation.

2.5. DiO or DiI Labeling of LDL

Human LDL (density 1.019-1.063 g/ml) was isolated by sequential ultracentrifugation from normolipidemic donors, dialyzed against saline-EDTA, and then sterilized by filtration through a 0.2-μm filter. Lipoproteins were labeled with DiO or DiI (Sigma) by incubating the LDL in 0.5% bovine serum albumin (BSA)/PBS with 100 ml DiO or DiI in DMSO (3 mg/ml) for 8 h at 37°C. The lipoproteins were then dialyzed against PBS and filtered before use.

2.6. Cell Transplantation and Immunosuppression

The protocols for cell transplantation and immunosuppression were described previously [12]. In brief, WHHL rabbits (8-week-old, purchased from Kitayamalabes, Ina, Nagano, Japan) were anesthetized with 50 mg/kg pentobarbital. An incision distal and parallel to the lower end of the ribcage was made, followed by a peritoneal incision and infusion of the ADMPC or control into the portal vein. The immunosuppression regimen consisted of the following: i) intramuscular injection of 6 mg/kg/day cyclosporin A daily from the day before surgery to sacrifice, ii) intramuscular injection of 0.05 mg/kg/day rapamycin daily from the day before surgery to sacrifice, iii) methylprednisolone at 3 mg/kg/day (day -1 to 7), followed by tapering to 2 mg/kg/day (day 8 to 14), 1 mg/kg/day (day 15 to 21), and 0.5 mg/kg/day (day 22 to the time at sacrifice), iv) intravenous injection of 20 mg/kg/day cyclophosphamide at days 0, 2, 5, and 7, and, v) intramuscular injection of 2.5 mg/kg/day ganciclovir to avoid viral infection in the immunocompromised host.

2.7. Immunohistochemical Staining of WHHL Rabbit Liver Sections

The WHHL livers were harvested and fixed immediately with 10% formalin. They were placed into optimal cutting temperature (OCT) compound (Sakura Finetechnical), frozen immediately, and then sectioned at 7 μm-thickness. The sections were incubated with blocking solution (Blocking one; Nacalai Tesque) for 1 h, and then incubated with rabbit anti-human albumin antibody (MBL, Nagoya, Japan) or mouse anti-human CD90 antibody followed by Alexa Fluor 488-labeled goat anti-rabbit IgG or Alexa Fluor 546-labeled goat anti-mouse IgG (Molecular Probes, Eugene, OR). The stained sections were examined with a BioZero laser scanning microscope (Keyence, Osaka, Japan).

Table 1. Differences Between ADMPC and ADSC of their Differentiation / Proliferation Abilities

	Self-Aggregation Properties	EDTA-Sensitiveness	Differentiation Abilities			Proliferation Abilities	
			Adipocytic	Osteocytic	Chondrocytic	After Reseeding	After Passaging
ADMPC	+	+	++	++	++	+	++
ADSC	-	-	+	+	+	++	++

2.8. PCR Analysis of WHHL Rabbit Liver for Human Liver-Specific Genes

Total RNAs of WHHL rabbit liver, hADMPC, and human hepatocytes were isolated using an RNAeasy kit (Qiagen, Valencia, CA). After treatment with DNase, the cDNAs were synthesized using Superscript III RNase H-minus Reverse Transcriptase (Invitrogen). Real-time PCR was performed using the ABI Prism 7900 Sequence Detection System (Applied Biosystems, Foster City, CA). 20X Assays-on-Demand™ Gene Expression Assay Mix for human alpha-1-antitrypsin (hAAT1) (Hs01097800_m1), human albumin (Hs00609411_m1), human Factor 9, human GATA4 (Hs00171403_m1), human hepatocyte nuclear factor 3beta (HNF-3beta) (Hs00232764_m1), human LDL receptor (Hs00181192_m1), and human glyceraldehyde-3-phosphate dehydrogenase (GAPDH) (Hs99999905_m1) were obtained from Applied Biosystems. It was confirmed that our human detectors and rabbit detectors did not cross-react with the other species. TaqMan® Universal PCR Master Mix and No AmpErase® UNG (2X) were also purchased from Applied Biosystems. Reactions were performed in quadruplicate and the mRNA levels were normalized relative to human GAPDH expression. To confirm that hADMPC differentiated into hepatocytes *in vivo*, the cells were tested by quantitative PCR before transplantation using human primary hepatocytes (Invitrogen, Lot number; HuP81) as controls.

2.9. Assay for Lipid Profiling

Serum samples were obtained from nonfasting rabbits before and after transplantation. Serum total cholesterol was measured in each sample using assay kits from Wako Pure Chemical Industries (Osaka, Japan). Serum lipoproteins were analyzed by an on-line dual enzymatic method for simultaneous quantification of cholesterol and triglycerides by high-performance liquid chromatography at Skylight Biotech (Akita, Japan), according to the described procedure [21].

2.10. Clearance of ^{125}I-LDL from Rabbit Serum

WHHL rabbits (8 weeks old) were anesthetized with pentobarbital (50 mg/kg). The peritoneum was incised and hADMPC (high-dose; 3 x 10^7 cells/rabbit, n = 2, low-dose; 5 x 10^6 cells/rabbit, n = 2) suspended in 3 ml of HBSS (20°C) (n = 5) or 3 ml of control (n = 2) were infused into the portal vein via an 18-gauge Angiocath™ (BD, UT). Eight weeks later, the animals were tested by the LDL turnover assay. ^{125}I-labeled human LDL (BT-913R, Biomedical Technologies, Stoughton, MA) was delivered via the marginal ear vein of the WHHL rabbits. Blood was collected from the opposite ear after injection at 5 min, 1 h, 2 h, 4 h, 6 h, and 28 h. ^{125}I-labeled apolipoprotein B-containing LDL was precipitated with 20% trichloroacetic acid (Wako Pure Chemical Industries) (serum; 320 µl, 100% w/v TCA 80 µl), and then the precipitants were applied for counting.

2.11. Statistical Analysis and Ethical Considerations

All animal studies described in this report were approved by Kobe University Graduate School of Medicine and Foundation for Biomedical Research and Innovation. Values were expressed as mean ± SEM. Differences between mean values of treated and untreated groups were evaluated using the Student's t-test. A P value less than 0.05 was considered statistically significant. All statistical analyses were performed using the SPSS Statistics 17.0 package (SPSS Inc., Chicago, IL).

3. RESULTS AND DISCUSSION

3.1. Self-Aggregation Properties and EDTA-Sensitivity of ADMPC

In the ADMPC isolation procedure were shown in Fig. (**1A**) (cited from reference 12 with modification). First, we removed contaminating red blood cells using density gradient centrifugation after digestion of adipose tissue to obtain the stromal vascular fraction (SVF). After 24-hour culture of the SVF (Fig. **1Aa**), adherent cells were treated with EDTA solution and the suspended cells were collected. Finally, these cells were re-plated on human FN-coated dishes (Fig. **1Ab**) and cultured (Fig. **1Ac**). Within 2–3 passages after the initial plating of the primary culture, ADMPC appeared as a monolayer of large flat cells (25–30 µm in diameter). As the cells approached confluence, they became spindle-shaped, resembling fibroblasts (Fig. **1Ad**). We next analyzed the mRNA expression levels of *islet-1* and *nkx2.5* in the two types of cells. *Islet-1* is a marker of undifferentiated cells and progenitors of cardiomyocytes, hepatocytes and pancreatic β cells, and *nkx2.5* is a marker of progenitors of cardiomyocytes. As shown in Fig. (**1B**), *islet-1* and *nkx2.5* were expressed in ADMPC, but not in ADSC. No or faint staining was noted for *GATA-4*, *myosin light chain*, *alpha cardiac actin*, and *myosin heavy chain* expression in both ADMPC and ADSC. On the other hand, flowcytometric analysis showed no significant different pattern in their cell surface markers between ADMPC and ADSC.

3.2. Adipocytic, Osteocytic and Chondrocytic Differentiation

In the next step, we assessed whether the adipocytic, osteocytic, and chondrocytic differentiation potentials of ADMPC were higher than those of ADSC (Table **1**). Adipo-

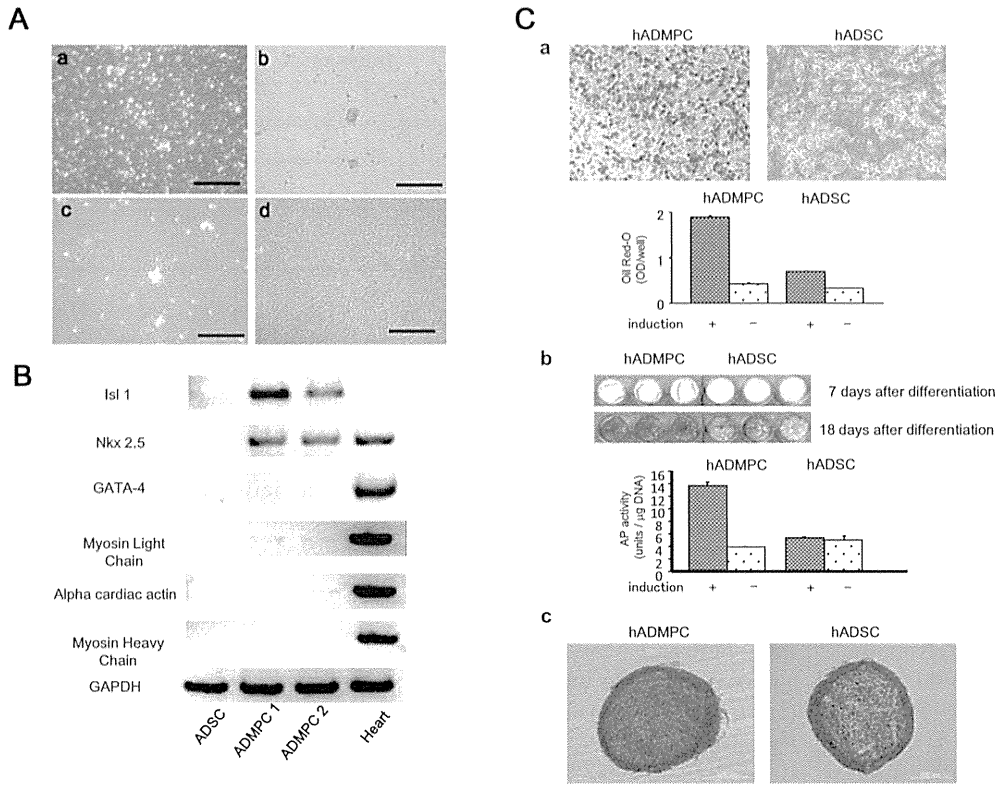

Fig. (1). Characters of ADMPC (**A**) Morphological characteristics of ADMPC. The cells obtained from adipose tissue were seeded and incubated for 24 h (a). Following incubation, the adherent cells were treated with EDTA solution, and the resulting suspended cells were replated at a density of 10,000 cells/cm^2 on human fibronectin (FN)-coated dishes (BD BioCoat) (b and c). Within 2–3 passages after the initial plating of the primary culture, ADMPC appeared as a monolayer of large flat cells (25–30 μm in diameter). As the cells approached confluence, they assumed a more spindle-shaped, fibroblastic morphology (d). Calibration bars = 500 μm (a, c and d) and 200 μm (b). Cited from reference 12 with modification. (**B**) Comparison of mRNA expression of markers of undifferentiated cells on ADMPC and ADSC. Islet-1, a marker of undifferentiated cells and progenitors of cardiomyocytes, hepatocytes, and pancreatic β cells, and nkx2.5, a transcription factor known to mark cardiomyocyte differentiation, were expressed in ADMPC, but not ADSC. GATA-4, a myosin light chain protein, α-cardiac actin, and myosin heavy chain protein were absent or only faintly stained in both cell types. Human heart mRNA was used as the control in these experiments. (**C**) Differences in the differentiation potentials between ADMPC and ADSC. (a) Morphological comparison of the adipogenic differentiation potential of ADMPC and ADSC. The cells were cultured in Differentiation Medium. After three days, half of the medium was replaced with adipocyte medium and this was repeated every two days. Five days after differentiation, the lipid contents of differentiated adipocytes were confirmed by Oil Red O staining. The lipid contents of differentiated adipocytes were confirmed by Oil Red O extraction. hADMPC showed higher lipid contents than hADSC. Data are mean ± SEM of triplicate experiments. (b) Morphological comparison of osteogenic differentiation potential of ADMPC and ADSC. At 7 or 18 days after osteogenic differentiation, the cells were stained with Alizarin red S for mineralized nodules. ADMPC showed higher osteogenic differentiation potential than ADSC. even days after osteogenic differentiation, the cells were assayed for alkaline phosphatase (APase) activity. AP activity per cell was calculated based on the amount of DNA. hADMPC showed higher APase activity than hADSC. Data are mean ± SEM of triplicate experiments. (c) Comparison of chondrogenic differentiation potential between ADMPC and ADSC. Extracellular matrices of differentiated ADMPC and ADSC into chondrocytes were visualized with Alcian Blue staining.

cytic differentiation was induced by culture with the Differentiation Medium containing 1-methyl-3-isobutylxanthine, dexamethasone, and insulin. Induction was confirmed by the accumulation of intracellular lipid droplets that could be stained with Oil Red O. The results showed higher levels of adipocytic induction for ADMPC than ADSC (Fig. **1Ca**). Next, osteocytic induction was examined by Alizarin red S staining (Fig. **1Cb**). After a 7-day induction for osteocytic differentiation, ADMPC only were stained with Alizarin red S. ADSC were stained after an 18-day induction, but their staining intensity lagged behind that of ADMPC (Fig. **1Cb**). Third, the chondrocytic differentiation potential of ADMPC and ADSC was compared. As shown in Fig. (**1Cc**), ADMPC showed more intense Alcian Blue staining than ADSC, suggesting higher chondrocytic induction for ADMPC than ADSC. The self-aggregation properties of ADMPC might introduce their higher chondrocytic induction than ADSC. These results indicated that ADMPC have higher differentiation potentials than ADSC.

3.3. *In Vitro* Differentiation of ADMPC into Hepatocytes

To obtain hepatocyte-like cell clusters, we have established a three-step method (Fig. **2A**). Immunofluorescence staining (Fig. **2B**) showed albumin- and alpha-1-antitrypsin-expressing cells among the differentiated ADMPC (cited from reference 10 with modification). The ability to secrete

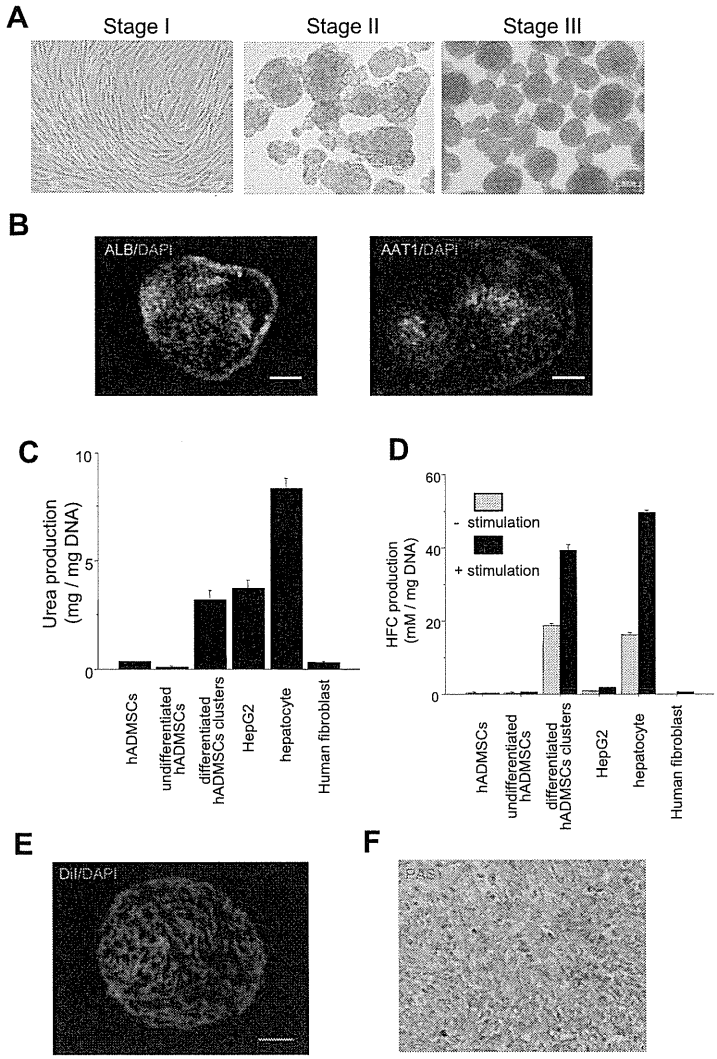

Fig (2). (**A**) General outline of the three-stage differentiation protocol. Stage I: growth of hADMSCs. Stage II: formation of cell clusters by culture in low osmotic medium on ultralow-attachment culture dishes. Stage III: growth factor stimulation of cell cluster cultures with bFGF, HGF, and OSM. DMSO was added on the 10th day after induction. (**B**) Immunofluorescence staining for ALB (left) and AAT (right) in differentiated ADMPC clusters. Scale bar, 100 mm. (**C**) Urea synthesis by differentiated ADMPC clusters after incubation with 5 mM NH_4Cl. Urea synthesis per cell was calculated based on the amount of DNA. Data are mean±SEM of triplicate experiments. (**D**) CYP enzyme activity in differentiated ADMPC clusters, as determined by hydroxylation of 7-benzyloxy-4-trifluoromethyo-coumarin to HFC. Before incubation with 100 mM, cells were cultured in the absence (non-stimulation) or presence (stimulation) of 10 mM rifampicin. CYP activity per cell was calculated based on the amount of DNA. Data are mean±SEM of triplicate experiments. (**E**) Low-density lipoprotein uptake by differentiated ADMPC clusters. Samples were examined by confocal laser scanning microscopy. Scale bar, 100 mm. (**F**) Glycogen storage in differentiated ADMPC clusters, as determined by PAS staining. hALB, human ALB; SEM, standard error of the mean; HFC, 7-hydroxy-4-trifluoromethyl-coumarin; PAS, periodic acid-Schiff's; DiI, 1,10-dioctadecyl-3,3,30,30-tetramethylindocarbocyanine; DAPI, 40,6-diamidino-2-phenylindole.

urea was about 12-fold higher for differentiated ADMPC incubated with NH_4Cl, compared with stage I undifferentiated ADMPC, and as high as that of HepG2 cells (Fig. **2C**). Nonfluorescent 7-benzyl-trifluoromethyl coumarin (BFC) is metabolized mainly by the cytochrome P450 (CYP) 3A family of enzymes and converted to the fluorescent 7-hydroxy-4-trifluoromethylcoumarin (HFC). The concentration of HFC in the supernatant was measured after incubation with 100 mM BFC. CYP activity in differentiated ADMPC clusters was 40-fold higher than in undifferentiated ADMPC (Fig. **2D**). In addition, CYP activity in differentiated ADMPC clusters increased 2–2.5-fold following preincubation with rifampicin for 3 days. In contrast, no increase in CYP activity was induced in undifferentiated ADMPC under this condition. We also assessed LDL uptake by differentiated ADMPC clusters by incubating differentiated ADMPC with DiI-LDL (Fig. **2E**). DiI-LDL was markedly incorporated into the cytosol of differentiated ADMPC. Another function of hepatocytes is glycogen production (glyconeogenesis), and PAS staining showed glycogen storage in differentiated ADMPC (Fig. **2F**). These results suggest that hepatogenic cytokines and floating culture could mimic the liver microenvironment and promote the differentiation of ADMPC into hepatocyte-like cells *in vitro*.

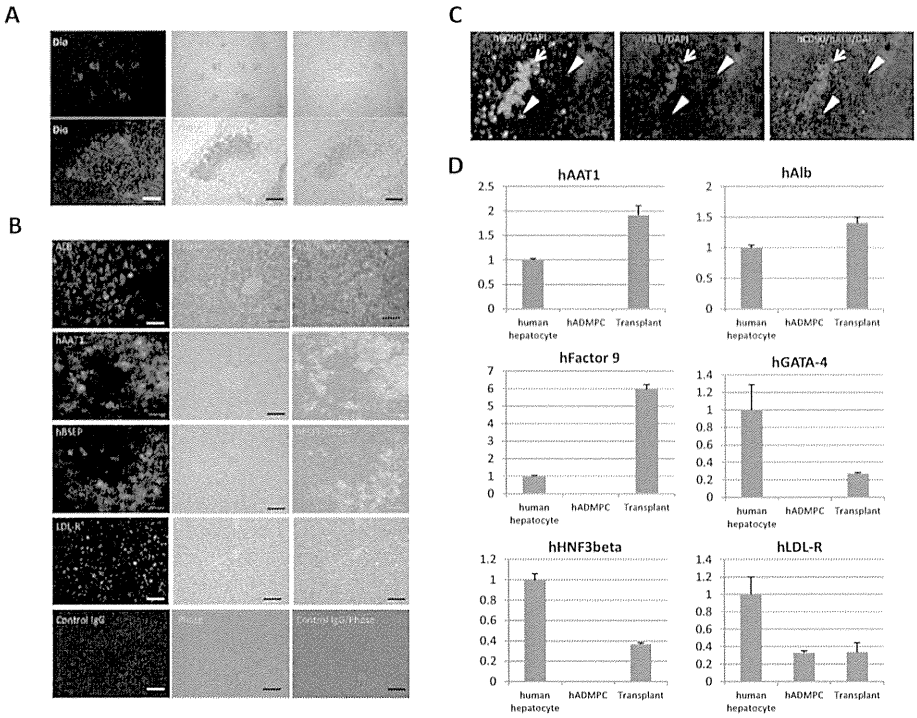

Fig (3). (A) Localization of transplanted hADMSCs in the WHHL liver. One week after transplantation of DiO-labeled hADMSCs via the portal vein, the WHHL rabbit liver was examined histologically. The DiO-labeled cells were localized in the portal area and dispersed in a centrilobular direction, resembling the mature innate hepatocytes. Bars = 200 μm (upper panels) and 100 μm (lower panels). (**B**) Immunohistochemical identification of human hepatocytic marker cells in liver sections of WHHL rabbits after ADMPC transplantation. Twelve weeks after ADMPC transplantation, human albumin-, human alpha-1-antitrypsin-, human bile salt export pump (BSEP)-, and LDL-receptor-positive cells were dispersed within the peri-venous regions of the liver parenchyma, where they made contact with and integrated among the host cells with cell-cell interactions between ADMPC-derived cells and diseased hepatocytes. Bar = 100 μm. (**C**) Differentiation of transplanted ADMPC into hepatocyte-like cells. Twelve weeks after transplantation, nearly all the human CD90-positive cells expressed human albumin, indicating that the major proportion of transplanted ADMPC could differentiate into hepatocyte-like cells (left panel: human CD90; middle panel: human albumin; right panel: merge). Arrows indicate human CD90 and human albumin double-positive cells; arrowheads indicate human CD90-positive/human albumin-negative cells. (**D**) Human hepatic gene expression in WHHL rabbit liver after ADMPC transplantation. RNA was prepared from WHHL rabbit livers 12 weeks after ADMPC transplantation. We examined expressions of the following hepatic markers by quantitative real time-polymerase chain reaction (RT-PCR) using the Assays-on-Demand Gene Expression Assay Mix: human alpha-1-antitrypsin, human albumin, human factor IX, human GATA-binding protein 4 (GATA-4), human hepatocyte nuclear factor 3 (HNF-3) beta, and human LDL-receptor. The livers of the control WHHL rabbits (saline, n = 3) were negative for all tested human hepatic genes. The mRNA levels were normalized based on human glyceraldehyde-3-phosphate dehydrogenase as a housekeeping gene and data are expressed as mean±SEM of triplicate experiments. The livers of ADMPC-recipient WHHL rabbits (n = 3) were positive for all tested human hepatic genes, which showed expression levels similar to those of human primary hepatocytes, but not ADMPC *per se*. Data are mean ± SEM.

3.4. *In Situ* Reprogramming of ADMPC into Hepatocytes

One week after transplantation of hADMPC via the portal vein, we examined whether the cells reside or not in the liver after transplantation. As shown in Fig. (**3A**), DiO-fluorescent labeled-hADMPC resided and distributed in the portal area, and morphologically resembled innate hepatocytes. Next, we should examine the recruitment of these cells directly into the rabbit liver and the success of hepatocytic differentiation. For this purpose, we measured human-specific hepatocytic proteins and their hepatic functions (Fig. **3**, cited from reference 12 with modification). Human albumin-, alpha-1-antitrypsin-, bile salt export pump-, and LDL-receptor-positive cells were dispersed within peri-venous regions of the liver parenchyma, where they had contacted and integrated among the host cells (Fig. **3B**). We also identified conserved cell-cell interactions between ADMPC-derived and diseased hepatocytes. To confirm this finding and to assess the efficacy of differentiation, we colocalized human CD90 and human albumin. As shown in Fig. (**3C**), nearly all human CD90-positive cells expressed human albumin, indicating that about 80% or more of transplanted ADMPC differentiated into human albumin-positive hepatocyte-like cells at 12 weeks after transplantation. Next, to confirm the differentiation of ADMPC into hepatocytes *in vivo*, the expression of hepatocyte markers was analyzed by quantitative RT-PCR. WHHL rabbit liver that was transplanted with ADMPC expressed higher levels of human-specific alpha-1-antitrypsin, albumin, and coagulation factor IX than control ADMPC (Fig. **3D**). The expression levels of human GATA-4, human hepatocyte nuclear factor 3 beta, and LDL-receptor were also higher in the WHHL rabbit liver than in the ADMPC untransplanted liver (Fig. **3D**). These results verified that ADMPC *per se* could differentiate into mature hepatocytes *in vivo*.

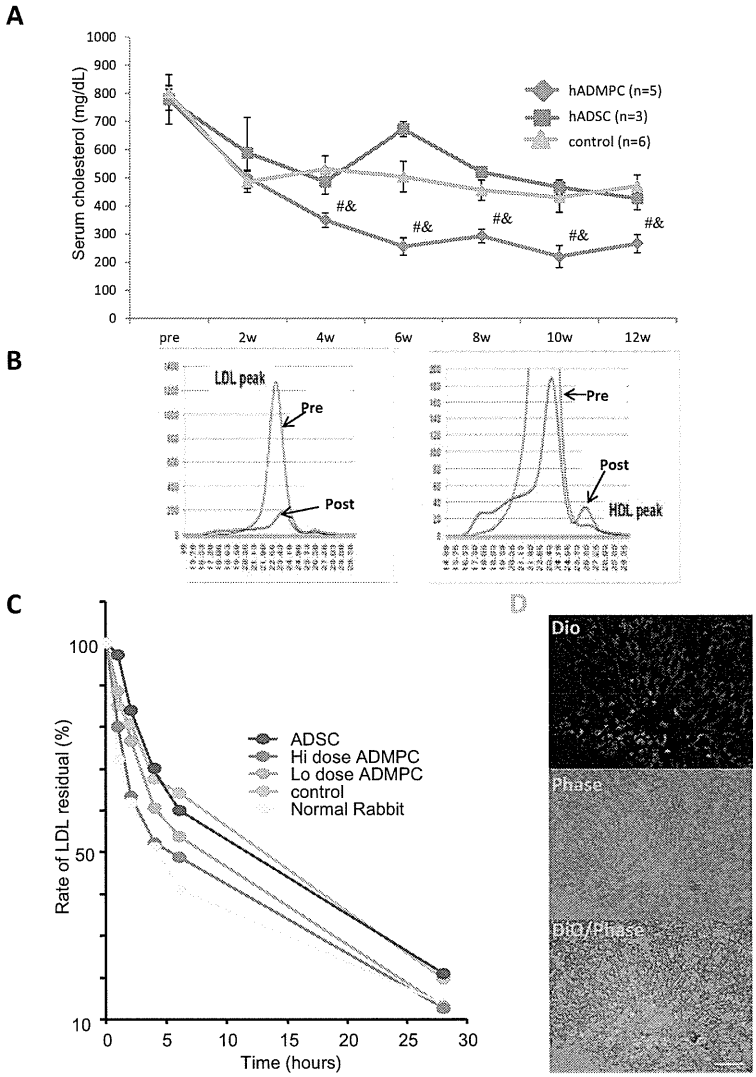

Fig. (4). (**A**) Total serum cholesterol levels. ADMPC transplantation in WHHL rabbits was followed for 12 weeks. Total serum cholesterol was measured in five rabbits that each received 3 x 10^7 ADMPC, three rabbits that each received 3 x 10^7 ADSC, and in six rabbits that received saline (control). Data are mean±SEM. #$P < 0.05$; control vs. the ADMPC-transplanted WHHL rabbit; &$P < 0.05$; the ADSC-transplanted WHHL rabbit vs. the ADMPC-transplanted WHHL rabbit). (**B**) Lipoprotein profiles in a representative WHHL rabbit with ADMP transplantation after gel filtration. Serum samples from the WHHL rabbit before and 4 weeks after transplantation were fractionated. Note the marked reduction in low-density lipoprotein (LDL) peak and appearance of a high-density lipoprotein (HDL) peak. (**C**) Rate of clearance of LDL from the serum of rabbits with and without transplantation of ADMPC. Animals were injected with ^{125}I-labeled human LDL, and the time course of clearance was monitored following trichloroacetic acid precipitation of serum at 5 min, 1 h, 2 h, 4 h, 6 h, and 28 h. Residual ^{125}I-LDL was expressed as a percentage of the signal at 5 min. The panel is the representative of two independent experiments. (**D**) DiO-LDL uptake into ADMPC-derived hepatocytes in the WHHL rabbit liver. Thin slices of recipient liver were incubated with DiO-labeled LDL in the serum-free medium for 24 h. After washing and fixation, the incubated slices were viewed by fluorescence microscopy. DiO-LDL-uptake cells (green) and no-uptake parenchymal cells are observed in the section. Bar = 100 μm.

3.5. *In Situ* Stem Cell Therapy by ADMPC

To determine the effects of ADMPC transplantation on the recipient rabbit lipid profile, serum cholesterol levels were monitored over 12 weeks (Fig. **4**, cited from reference 12 with modification). Significant reductions in total serum cholesterol were observed within 4 weeks of the transplantation, and the reductions were maintained for the entire period (Fig. **4A**). Furthermore, ADMPC-recipient animals showed significantly greater reductions than those in the control group. To determine the effects of ADMPC transplantation on the fractions of high-density lipoprotein and LDL in recipient animals, fractionation by fast protein liquid chromatography was performed (Fig. **4B**). Transplantation of ADMPC resulted in marked reduction of the peak LDL cholesterol and increment of high-density lipoprotein cholesterol fraction (right panel). Next, clearance experiments were performed with human LDL to confirm that the transplanted ADMPC contributed to the fall in serum cholesterol through uptake of LDL via LDL receptors. The rate of LDL clearance was significantly higher in the WHHL rabbits with transplanted ADMPC than WHHL rabbits without transplanted ADMPC (Fig. **4C**). Rabbits with ADMPC transplants showed ~2.4-fold (high-dose; 3 x 10^7 cells/rabbit) and

1.4-fold (low-dose; 5 x 10^6 cells/rabbit) increases in the rate of LDL cholesterol clearance over non-transplanted rabbits. To evaluate the uptake of DiO-LDL by transplants *ex vivo*, thin liver slices of WHHL rabbit were incubated with DiO-labeled LDL for 24 h and the uptake was examined as for the clearance experiments (Fig. **4D**). DiO-LDL was taken up by some but not all of the cells in the WHHL rabbit liver transplanted with ADMPC, with the positive cells observed dispersed, contacting, and integrating among the non DiO-LDL-positive parenchymal cells. This finding suggests that ADMPC differentiated into hepatocytes *in vivo*, thus lowering the serum cholesterol directly via LDL uptake.

3.6. ADMPC as a Promising Tool for Regenerative Medicine

For any successful regenerative medicine program, three issues must be considered: 1) what kind of tissues should be nominated as cell sources, 2) how should the cells be obtained from tissues, and 3) how will the cells behave after transplantation/administration. The following section discusses these considerations with respect to this study.

The source of stem cells for regenerative medicine should be easily and safely accessible as well as free of any ethical issues, thus allowing allogenic as well as autologous cellular therapy applications, and finally, the cell source should be available in large amounts. Adipose tissue is therefore a suitable cell source under these criteria. Liposuction surgery provides a safe method for collection of adipose tissue, harvesting from 100 ml to >3 L of lipoaspirate from material that is routinely discarded, thus avoiding any ethical concerns [16].

As to the second issue of cell processing, methods to isolate cells from adipose tissue were first reported in the 1960s [17-19]. Such methods involved mincing rat fat pads and incubating the resultant tissue fragments with collagenase. The digested material was then centrifuged to separate the floating population of mature adipocytes from the pelleted stromal vascular fraction (SVF). The SVF, which are sometimes referred to adipose tissue-derived regenerative cells (ADRC), consists of a heterogeneous cell population including fibroblasts, endothelial cells, pre-adipocytes, and mesenchymal stem cells [17-19]. However, as mentioned, this non-cultured cell population is too heterogeneous to apply therapeutically, necessitating the isolation of pre-adipocyte and/or mesenchymal stem cell-rich adherent cells from the SVF. The original procedure for this separation step was subsequently modified for the isolation of cells from human adipose tissue SVFs [20-23], and Zuk *et al.* [7] reported that the processed lipoaspirates exhibited mesenchymal stem cell-like features and could differentiate into adipocytes, osteocytes, and chondrocytes. Such cells are currently labeled as adipose tissue-derived stem cells (ADSC). The procedure used for obtaining these stem cells from lipoaspirates was described by Bjorntorp *et al.* [24] to obtain pre-adipocytes.

We have subsequently developed a novel isolation method for stem-like cells according to their adhesion properties [8-12]. As shown in Fig. (**1Aa**), fibroblast- and endothelial-like cells completely adhered onto the culture dish after 24 h in culture following the first-plating of the SVF. Most of the SVF cells were difficult to detach by conventional pipetting after this length of culture (24 h). However, a population of round self-aggregating cells that could only be detached by treatment with EDTA solution showed multi-lineage differentiation potency. In the EDTA-treating method, only cells of their properties with self-aggregation and EDTA-sensitiveness could be selected as ADMPC from plated SVF. In the conventional pre-plating methods to obtain ADSC [7, 24], the cells with EDTA-resistance could not be excluded. ADMPC exhibited high differentiation capacities for osteocytic, adipocytic, and chondrocytic lineages compared with ADSC, and could differentiate into hepatocyte-like cells, insulin-producing cells, and cardiomyoblast-like cells *in vitro* as non-mesenchymal lineages. We therefore named these cells ADMPC.

ADMPC differ from ADSC with regard to gene expression profiling. ADMPC express islet-1, a marker of undifferentiated cells and of cardiac, hepatic, and pancreatic progenitor cells [9-11]. Based on our findings, we propose that the islet-1-expressing ADMPC could be differentiated or reprogrammed into hepatocytes in the recipient liver *in vivo* after transplantation. In other words, the appropriate cells can show *in situ reprogramming* when transplanted and recruited into an appropriate environment.

Finally, we considered how the ADMPC would behave after transplantation/administration *in situ*. Traditionally, stem/progenitor cells are differentiated into terminally differentiated cells prior to transplantation/administration. For example, iPS cells are differentiated into neuronal cells and then applied for neuronal disease therapies. In these processes, researchers could mimic the relevant microenvironment and then differentiate the transplanted cells into the desired cell lineages. In contrast, we hypothesized that *in vitro* or *ex vivo* reprogramming could not sufficiently recapitulate the desired transplant microenvironment. Our concept is that the microenvironment *in situ* might supply cytokines to exert paracrine effects and form appropriate extracellular matrices, thus prompting the progenitor cells toward the desired terminal differentiation. ADMPC express islet-1, indicating that they might be appropriate progenitor cells on their own for *in situ* reprogramming as hepatocytes in the liver microenvironment. If these reprogrammed cells could correct given disease defects, clinical applications for *in situ* stem cell therapy become feasible.

In this review, we propose *in situ* stem cell therapy as a new tool for regenerative medicine and *in situ* reprogramming as a mechanism for the correction of disease. Yamanaka *et al.* [25] presented terminally differentiated cells that could be reprogrammed into the pluripotent state using only four factors. Followers confirmed the fact and named the concept "reprogramming". Melton *et al.* [26] subsequently showed that gene-modified cells alone could direct differentiation along a terminal path, and renamed the mechanism "direct reprogramming", and some cases of *ex vivo* gene therapy might be included in this concept. Here, we presented stem-like cells that could differentiate terminally *in situ* in the appropriate microenvironment.

4. CONCLUSIONS

In this review we describe ADMPC, novel adipose tissue-derived cells with stem cell-like properties and higher

differentiation potential than previously reported adipose tissue-derived cells. Not only could ADMPC differentiate into hepatocyte-like cells *in vitro*, but ADMPC *per se* also showed the same capacity in the hepatic environment and the *in situ* reprogrammed cells could correct the metabolic defect of diseased animals. The mechanisms described for *in situ* reprogramming hold great promise for applications in regenerative medicine as "*in situ* stem cell therapy".

CONFLICT OF INTEREST

The authors confirm that this article content has no conflicts of interest.

ACKNOWLEDGEMENTS

This study was supported in part by the Program for Promotion of Fundamental Studies in Health Sciences of the National Institute of Biomedical Innovation (NIBIO) and Kobe Translational Research Cluster, the Knowledge Cluster Initiative, Ministry of Education, Culture, Sports, Science and Technology (MEXT).

DISCLOSURE

It should be noted that the authors have previously published much of the material covered in this review article in "Tissue Eng Part C Methods", Volume 17, 2011, Pages 145-154.

REFERENCES

[1] Wagers AJ, Weissman IL. Plasticity of adult stem cells. Cell 2004; 116: 639-48.

[2] Pittenger MF, Mackay AM, Beck SC, *et al.* Multilineage potential of adult human mesenchymal stem cells. Science 1999; 284: 143-7.

[3] Shih DT, Lee DC, Chen SC, *et al.* Isolation and characterization of neurogenic mesenchymal stem cells in human scalp tissue. Stem Cells 2005; 23: 1012-20.

[4] In 't Anker PS, Scherjon SA, Kleijburg-van der Keur C, *et al.* Isolation of mesenchymal stem cells of fetal or maternal origin from human placenta. Stem Cells 2004; 22: 1338-45.

[5] Bieback K, Kern S, Klüter H, Eichler H. Critical parameters for the isolation of mesenchymal stem cells from umbilical cord blood. Stem Cells 2004; 22: 625-34.

[6] Jiang Y, Jahagirdar BN, Reinhardt RL, *et al.* Pluripotency of mesenchymal stem cells derived from adult marrow. Nature 2002; 418: 41-9.

[7] Zuk PA, Zhu M, Ashjian P, *et al.* Human adipose tissue is a source of multipotent stem cells. Mol Biol Cell 2002; 13: 4279-95.

[8] Komoda H, Okura H, Lee C-M, *et al.* Reduction of Neu5GC xenoantigen on human ADMSCs lead to them as safer and more useful cell sources for realizing various stem cell therapies. Tissue Eng Part A 2010; 16: 1143-55.

[9] Okura H, Matsuyama A, Lee CM, *et al.* Cardiomyoblast-like cells differentiated from human adipose tissue-derived mesenchymal stem cells improve left ventricular dysfunction and survival in a rat myocardial infarction model. Tissue Eng Part C Methods 2010; 16: 417-25.

[10] Okura H, Komoda H, Saga A, *et al.* Properties of hepatocyte-like cell clusters from human adipose tissue-derived mesenchymal stem cells. Tissue Eng Part C Methods 2010; 16: 761-70.

[11] Okura H, Fumimoto Y, Komoda H, *et al.* Transdifferentiation of human adipose tissue-derived stromal cells into insulin-producing clusters. J Artif Organs 2009; 12: 123-30.

[12] Okura H, Saga A, Fumimoto Y, *et al.* Transplantation of human adipose tissue-derived multilineage progenitor cells reduces serum cholesterol in hyperlipidemic Watanabe rabbits. Tissue Eng Part C Methods 2011; 17: 145-54.

[13] Saga A, Okura H, Soeda M, *et al.* HMG-CoA reductase inhibitor augments the serum total cholesterol-lowering effect of human adipose tissue-derived multilineage progenitor cells in hyperlipidemic homozygous Watanabe rabbits. Biochem Biophys Res Commun 2011; 412: 50-4.

[14] Hosono T, Mizuguchi H, Katayama K, *et al.* RNA interference of PPARgamma using fiber-modified adenovirus vector efficiently suppresses preadipocyte-to-adipocyte differentiation in 3T3-L1 cells. Gene 2005; 348: 157-65.

[15] Yanagita M, Kashiwagi Y, Kobayashi R, Tomoeda M, Shimabukuro Y, Murakami S. Nicotine inhibits mineralization of human dental pulp cells. J Endod 2008; 34: 1061-5.

[16] Katz AJ, Llull R, Hedrick MH, Futrell JW. Emerging approaches to the tissue engineering of fat. Clin Plast Surg 1999; 26: 587-603.

[17] Rodbell M. Metabolism of isolated fat cells. II. The similar effects of phospholipase c (*Clostridium perfringens* alpha toxin) and of insulin on glucose and amino acid metabolism. J Biol Chem 1966; 241: 130-9.

[18] Rodbell M. The metabolism of isolated fat cells. IV. Regulation of release of protein by lipolytic hormones and insulin. J Biol Chem 1966; 241: 3909-17.

[19] Rodbell M, Jones AB. Metabolism of isolated fat cells. III. The similar inhibitory action of phospholipase c (clostridium perfringens alpha toxin) and of insulin on lipolysis stimulated by lipolytic hormones and theophylline. J Biol Chem 1966; 241: 140-2.

[20] Van RL, Bayliss CE, Roncari DA. Cytological and enzymological characterization of adult human adipocyte precursors in culture. J Clin Invest 1976; 58: 699-704.

[21] Björntorp P, Karlsson M, Gustafsson L, *et al.* Quantitation of different cells in the epididymal fat pad of the rat. J Lipid Res 1979; 20: 97-106.

[22] Deslex S, Negrel R, Vannier C, Etienne J, Ailhaud G. Differentiation of human adipocyte precursors in a chemically defined serum-free medium. Int J Obes 1987; 11: 19-27.

[23] Hauner H, Entenmann G, Wabitsch M, *et al.* Promoting effect of glucocorticoids on the differentiation of human adipocyte precursor cells cultured in a chemically defined medium. J Clin Invest 1989; 84: 1663-70.

[24] Bjorntorp P, Karlsson M, Pertoft H, Pettersson P, Sjostrom L, Smith U. Isolation and characterization of cells from rat adipose tissue developing into adipocytes. J Lipid Res 1978; 19: 316-24.

[25] Yamanaka S. Strategies and new developments in the generation of patient-specific pluripotent stem cells. Cell Stem Cell 2007; 1: 39-49.

[26] Gurdon JB, Melton DA. Nuclear reprogramming in cells. Science 2008; 322: 1811-5.

Received: October 24, 2011 Revised: December 2, 2011 Accepted: January 3, 2012

Research Article

EASL EUROPEAN ASSOCIATION FOR THE STUDY OF THE LIVER | JOURNAL OF HEPATOLOGY

Generation of metabolically functioning hepatocytes from human pluripotent stem cells by FOXA2 and HNF1α transduction

Kazuo Takayama[1,2], Mitsuru Inamura[1,2], Kenji Kawabata[2,3], Michiko Sugawara[4], Kiyomi Kikuchi[4], Maiko Higuchi[2], Yasuhito Nagamoto[1,2], Hitoshi Watanabe[1,2], Katsuhisa Tashiro[2], Fuminori Sakurai[1], Takao Hayakawa[5,6], Miho Kusuda Furue[7,8], Hiroyuki Mizuguchi[1,2,9,*]

[1]*Laboratory of Biochemistry and Molecular Biology, Graduate School of Pharmaceutical Sciences, Osaka University, Osaka 565-0871, Japan;* [2]*Laboratory of Stem Cell Regulation, National Institute of Biomedical Innovation, Osaka 567-0085, Japan;* [3]*Laboratory of Biomedical Innovation, Graduate School of Pharmaceutical Sciences, Osaka University, Osaka 565-0871, Japan;* [4]*Tsukuba Laboratories, Eisai Co., Ltd., Ibaraki 300-2635, Japan;* [5]*Pharmaceutics and Medical Devices Agency, Tokyo 100-0013, Japan;* [6]*Pharmaceutical Research and Technology Institute, Kinki University, Osaka 577-8502, Japan;* [7]*Laboratory of Cell Cultures, Department of Disease Bioresources Research, National Institute of Biomedical Innovation, Osaka 567-0085, Japan;* [8]*Laboratory of Cell Processing, Institute for Frontier Medical Sciences, Kyoto University, Kyoto 606-8507, Japan;* [9]*The Center for Advanced Medical Engineering and Informatics, Osaka University, Osaka 565-0871, Japan*

Background & Aims: Hepatocyte-like cells differentiated from human embryonic stem cells (hESCs) and induced pluripotent stem cells (hiPSCs) can be utilized as a tool for screening for hepatotoxicity in the early phase of pharmaceutical development. We have recently reported that hepatic differentiation is promoted by sequential transduction of SOX17, HEX, and HNF4α into hESC- or hiPSC-derived cells, but further maturation of hepatocyte-like cells is required for widespread use of drug screening.
Methods: To screen for hepatic differentiation-promoting factors, we tested the seven candidate genes related to liver development.
Results: The combination of two transcription factors, FOXA2 and HNF1α, promoted efficient hepatic differentiation from hESCs and hiPSCs. The expression profile of hepatocyte-related genes (such as genes encoding cytochrome P450 enzymes, conjugating enzymes, hepatic transporters, and hepatic nuclear receptors) achieved with FOXA2 and HNF1α transduction was comparable to that obtained in primary human hepatocytes. The hepatocyte-like cells generated by FOXA2 and HNF1α transduction exerted various hepatocyte functions including albumin and urea secretion, and the uptake of indocyanine green and low density lipoprotein. Moreover, these cells had the capacity to metabolize all nine tested drugs and were successfully employed to evaluate drug-induced cytotoxicity.
Conclusions: Our method employing the transduction of FOXA2 and HNF1α represents a useful tool for the efficient generation of metabolically functional hepatocytes from hESCs and hiPSCs, and the screening of drug-induced cytotoxicity.

Keywords: FOXA2; HNF1α; Hepatocytes; Adenovirus; Drug screening; Drug metabolism; hESCs; hiPSCs.
Received 14 November 2011; received in revised form 31 March 2012; accepted 4 April 2012; available online 29 May 2012
* Corresponding author. Address: Laboratory of Biochemistry and Molecular Biology, Graduate School of Pharmaceutical Sciences, Osaka University, 1-6 Yamadaoka, Suita, Osaka 565-0871, Japan. Tel.: +81 6 6879 8185; fax: +81 6 6879 8186.
E-mail address: mizuguch@phs.osaka-u.ac.jp (H. Mizuguchi).

Introduction

Hepatocyte-like cells differentiated from human embryonic stem cells (hESCs) [1] or human induced pluripotent stem cells (hiPSCs) [2] have more advantages than primary human hepatocytes (PHs) for drug screening. While application of PHs in drug screening has been hindered by lack of cellular growth, loss of function, and de-differentiation *in vitro* [3], hESC- or hiPSC-derived hepatocyte-like cells (hESC-hepa or hiPSC-hepa, respectively) have potential to solve these problems.

Hepatic differentiation from hESCs and hiPSCs can be divided into four stages: definitive endoderm (DE) differentiation, hepatic commitment, hepatic expansion, and hepatic maturation. Various growth factors are required to mimic liver development [4] and to promote hepatic differentiation. Previously, we showed that transduction of transcription factors in addition to treatment with optimal growth factors was effective to enhance hepatic differentiation [5–7]. An almost homogeneous hepatocyte population was obtained by sequential transduction of SOX17, HEX, and HNF4α into hESC- or hiPSCs-derived cells [7]. However, further maturation of the hESC-hepa and hiPSC-hepa is required for widespread use of drug screening because the drug metabolism capacity of these cells was not sufficient.

In some previous reports, hESC-hepa and hiPSC-hepa have been characterized for their hepatocyte functions in numerous ways, including functional assessment such as glycogen storage and low density lipoprotein (LDL) uptake [7]. To make a more precise judgment as to whether hESC-hepa and hiPSC-hepa can be applied to drug screening, it is more important to assess cytochrome P450 (CYP) induction potency and drug metabolism capacity rather than general hepatocyte function. Although Duan *et al.* have examined the drug metabolism capacity of hESC-hepa, drug metabolites were measured at 24 or 48 h [8]. To precisely

estimate the drug metabolism capacity, the amount of metabolites must be measured during the time when production of metabolites is linearly detected (generally before 24 h). To the best of our knowledge, there have been few reports that have examined various drugs metabolism capacity of hESC-hepa and hiPSC-hepa in detail.

In the present study, seven candidate genes (*FOXA2*, *HEX*, *HNF1α*, *HNF1β*, *HNF4α*, *HNF6*, and *SOX17*) were transduced into each stage of hepatic differentiation from hESCs by using an adenovirus (Ad) vector to screen for hepatic differentiation-promoting factors. Then, hepatocyte-related gene expression profiles and hepatocyte functions in hESC-hepa and hiPSC-hepa generated by the optimized protocol, were examined to investigate whether these cells have PHs characteristics. We used nine drugs, which are metabolized by various CYP enzymes and UDP-glucuronosyltransferases (UGTs), to determine whether the hESC-hepa and hiPSC-hepa have drug metabolism capacity. Furthermore, hESC-hepa and hiPSC-hepa were examined to determine whether these cells may be applied to evaluate drug-induced cytotoxicity.

Materials and methods

In vitro differentiation

Before the initiation of cellular differentiation, the medium of hESCs and hiPSCs was exchanged for a defined serum-free medium, hESF9, and cultured as previously reported [9]. The differentiation protocol for the induction of DE cells, hepatoblasts, and hepatocytes was based on our previous report with some modifications [5,6]. Briefly, in mesendoderm differentiation, hESCs and hiPSCs were dissociated into single cells by using Accutase (Millipore) and cultured for 2 days on Matrigel (BD biosciences) in differentiation hESF-DIF medium which contains 100 ng/ml Activin A (R&D Systems) and 10 ng/ml bFGF (hESF-DIF medium, Cell Science & Technology Institute; differentiation hESF-DIF medium was supplemented with 10 μg/ml human recombinant insulin, 5 μg/ml human apotransferrin, 10 μM 2-mercaptoethanol, 10 μM ethanolamine, 10 μM sodium selenite, and 0.5 mg/ml bovine serum albumin, all from Sigma). To generate DE cells, mesendoderm cells were transduced with 3000 VP/cell of Ad-FOXA2 for 1.5 h on day 2 and cultured until day 6 on Matrigel in differentiation hESF-DIF medium supplemented with 100 ng/ml Activin A and 10 ng/ml bFGF. For induction of hepatoblasts, the DE cells were transduced with each 1500 VP/cell of Ad-FOXA2 and Ad-HNF1α for 1.5 h on day 6 and cultured for 3 days on Matrigel in hepatocyte culture medium (HCM, Lonza) supplemented with 30 ng/ml bone morphogenetic protein 4 (BMP4, R&D Systems) and 20 ng/ml FGF4 (R&D Systems). In hepatic expansion, the hepatoblasts were transduced with each 1500 VP/cell of Ad-FOXA2 and Ad-HNF1α for 1.5 h on day 9 and cultured for 3 days on Matrigel in HCM supplemented with 10 ng/ml hepatocyte growth factor (HGF), 10 ng/ml FGF1, 10 ng/ml FGF4, and 10 ng/ml FGF10 (all from R&D Systems). In hepatic maturation, cells were cultured for 8 days on Matrigel in L15 medium (Invitrogen) supplemented with 8.3% tryptose phosphate broth (BD biosciences), 10% FBS (Vita), 10 μM hydrocortisone 21-hemisuccinate (Sigma), 1 μM insulin, 25 mM $NaHCO_3$ (Wako), 20 ng/ml HGF, 20 ng/ml Oncostatin M (OsM, R&D systems), and 10^{-6} M Dexamethasone (DEX, Sigma).

Results

Recently, we showed that the sequential transduction of SOX17, HEX, and HNF4α into hESC-derived mesendoderm, DE, and hepatoblasts, respectively, leads to efficient generation of the hESC-hepa [5–7]. In the present study, to further improve the differentiation efficiency towards hepatocytes, we screened for hepatic differentiation-promoting transcription factors. Seven candidate genes involved in liver development were selected. We then examined the function of the hESC-hepa and hiPSC-hepa generated by the optimized protocol for pharmaceutical use in detail.

Efficient hepatic differentiation by Ad-FOXA2 and Ad-HNF1α transduction

To perform efficient DE differentiation, T-positive hESC-derived mesendoderm cells (day 2) (Supplementary Fig. 1) were transduced with Ad vector expressing various transcription factors (Ad-FOXA2, Ad-HEX, Ad-HNF1α, Ad-HNF1β, Ad-HNF4α, Ad-HNF6, and Ad-SOX17 were used in this study). We ascertained the expression of *FOXA2*, *HEX*, *HNF1α*, *HNF1β*, *HNF4α*, *HNF6*, or *SOX17* in Ad-FOXA2-, Ad-HEX-, Ad-HNF1α-, Ad-HNF1β-, Ad-HNF4α-, Ad-HNF6-, or Ad-SOX17-transduced cells, respectively (Supplementary Fig. 2). We also verified that there was no cytotoxicity of the cells transduced with Ad vector until the total amount of Ad vector reached 12,000 VP/cell (Supplementary Fig. 3). Each transcription factor was expressed in hESC-derived mesendoderm cells on day 2 by using Ad vector, and the efficiency of DE differentiation was examined (Fig. 1A). The DE differentiation efficiency based on CXCR4-positive cells was the highest when Ad-SOX17 or Ad-FOXA2 were transduced (Fig. 1B). To investigate the difference between Ad-FOXA2-transduced cells and Ad-SOX17-transduced cells, gene expression levels of markers of undifferentiated cells, mesendoderm cells, DE cells, and extraembryonic endoderm cells were examined (Fig. 1C). The expression levels of extraembryonic endoderm markers of Ad-SOX17-transduced cells were higher than those of Ad-FOXA2-transduced cells. Therefore, we concluded that FOXA2 transduction is suitable for use in selective DE differentiation.

To promote hepatic commitment, various transcription factors were transduced into DE cells and the resulting phenotypes were examined on day 9 (Fig. 1D). Nearly 100% of the population of Ad-FOXA2-transduced cells and Ad-HNF1α-transduced cells was α-fetoprotein (AFP)-positive (Fig. 1E). We expected that hepatic commitment would be further accelerated by combining FOXA2 and HNF1α transduction. The DE cells were transduced with both Ad-FOXA2 and Ad-HNF1α, and then the gene expression levels of *CYP3A7* [10], which is a marker of fetal hepatocytes, were evaluated (Fig. 1F). When both Ad-FOXA2 and Ad-HNF1α were transduced into DE cells, the promotion of hepatic commitment was greater than in Ad-FOXA2-transduced cells or Ad-HNF1α-transduced cells.

To promote hepatic expansion and maturation, we transduced various transcription factors into hepatoblasts on day 9 and 12 and the resulting phenotypes were examined on day 20 (Fig. 1G). We ascertained that the hepatoblast population was efficiently expanded by addition of HGF, FGF1, FGF4, and FGF10 (Supplementary Fig. 4). The hepatic differentiation efficiency based on asialoglycoprotein receptor 1 (ASGR1)-positive cells was measured on day 20, demonstrating that FOXA2, HNF1α, and HNF4α transduction could promote efficient hepatic maturation (Fig. 1H). To investigate the phenotypic difference between Ad-FOXA2-, Ad-HNF1α-, and Ad-HNF4α-transduced cells, gene expression levels of early hepatic markers, mature hepatic markers, and biliary markers were examined (Fig. 1I). Gene expression levels of mature hepatic markers were up-regulated by FOXA2, HNF1α, or HNF4α transduction. FOXA2 transduction strongly upregulated gene expression levels of both early hepatic markers and mature hepatic markers, while HNF1α or HNF4α transduc-

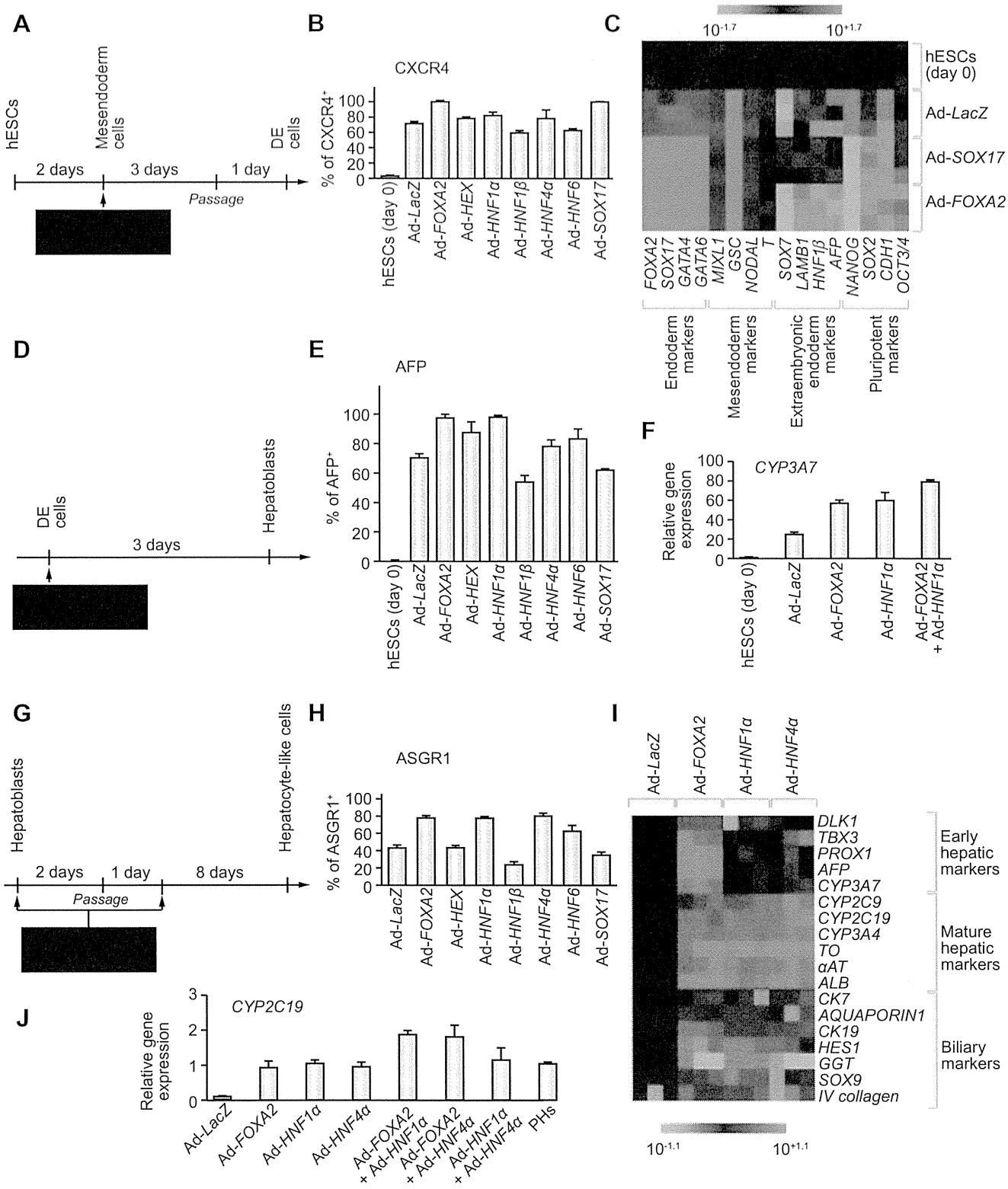

Fig. 1. Efficient hepatic differentiation from hESCs by FOXA2 and HNF1α transduction. (A) The schematic protocol describes the strategy for DE differentiation from hESCs (H9). Mesendoderm cells (day 2) were transduced with 3000 VP/cell of transcription factor (TF)-expressing Ad vector (Ad-TF) for 1.5 h and cultured as described in Fig. 2A. (B) On day 5, the efficiency of DE differentiation was measured by estimating the percentage of CXCR4-positive cells using FACS analysis. (C) The gene expression profiles were examined on day 5. (D) Schematic protocol describing the strategy for hepatoblast differentiation from DE. DE cells (day 6) were transduced with 3000 VP/cell of Ad-TF for 1.5 h and cultured as described in Fig. 2A. (E) On day 9, the efficiency of hepatoblast differentiation was measured by estimating the percentage of AFP-positive

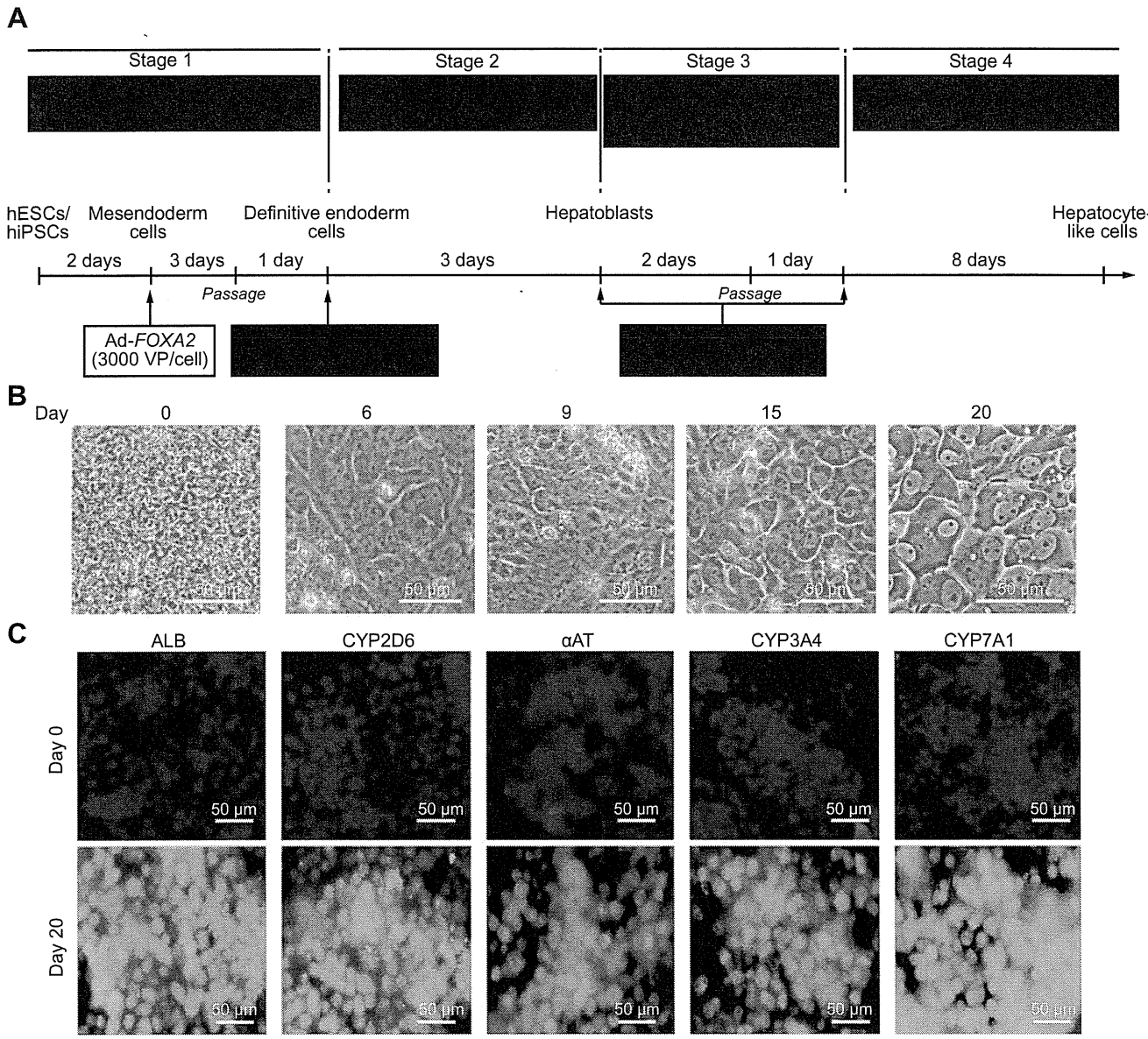

Fig. 2. Hepatic differentiation of hESCs and hiPSCs by FOXA2 and HNF1α transduction. (A) The differentiation procedure of hESCs and hiPSCs into hepatocytes via DE cells and hepatoblasts is schematically shown. Details of the hepatic differentiation procedure are described in Materials and methods. (B) Sequential morphological changes (day 0–20) of hESCs (H9) differentiated into hepatocytes are shown. (C) The expression of the hepatocyte markers (ALB, CYP2D6, αAT, CYP3A4, and CYP7A1, all green) was examined by immunohistochemistry on day 0 and 20. Nuclei were counterstained with DAPI (blue).

tion did not up-regulate the gene expression levels of early hepatic markers. Next, multiple transduction of transcription factors was performed to promote further hepatic maturation. The combination of Ad-FOXA2 and Ad-HNF1α transduction and the combination of Ad-FOXA2 and Ad-HNF4α transduction result in the most efficient hepatic maturation, judged from the gene expression levels of *CYP2C19* (Fig. 1J). This may happen because the mixture of immature hepatocytes and mature hepatocytes coor-

cells using FACS analysis. (F) The gene expression level of *CYP3A7* was measured by real-time RT-PCR on day 9. On the *y* axis, the gene expression level of *CYP3A7* in hESCs (day 0) was taken as 1.0. (G) The schematic protocol describes the strategy for hepatic differentiation from hepatoblasts. Hepatoblasts (day 9) were transduced with 3000 VP/cell of Ad-TF for 1.5 h and cultured as described in Fig. 2A. (H) On day 20, the efficiency of hepatic differentiation was measured by estimating the percentage of ASGR1-positive cells using FACS analysis. The detail results of FACS analysis are shown in Supplementary Table 1. (I) Gene expression profiles were examined on day 20. (J) Hepatoblasts (day 9) were transduced with 3000 VP/cell of Ad-TFs (in the case of combination transduction of two types of Ad vector, 1500 VP/cell of each Ad-TF was transduced) for 1.5 h and cultured. Gene expression levels of *CYP2C19* were measured by real-time RT-PCR on day 20. On the *y* axis, the gene expression level of *CYP2C19* in PHs, which were cultured for 48 h after the cells were plated, was taken as 1.0. All data are represented as mean ± SD (n = 3).

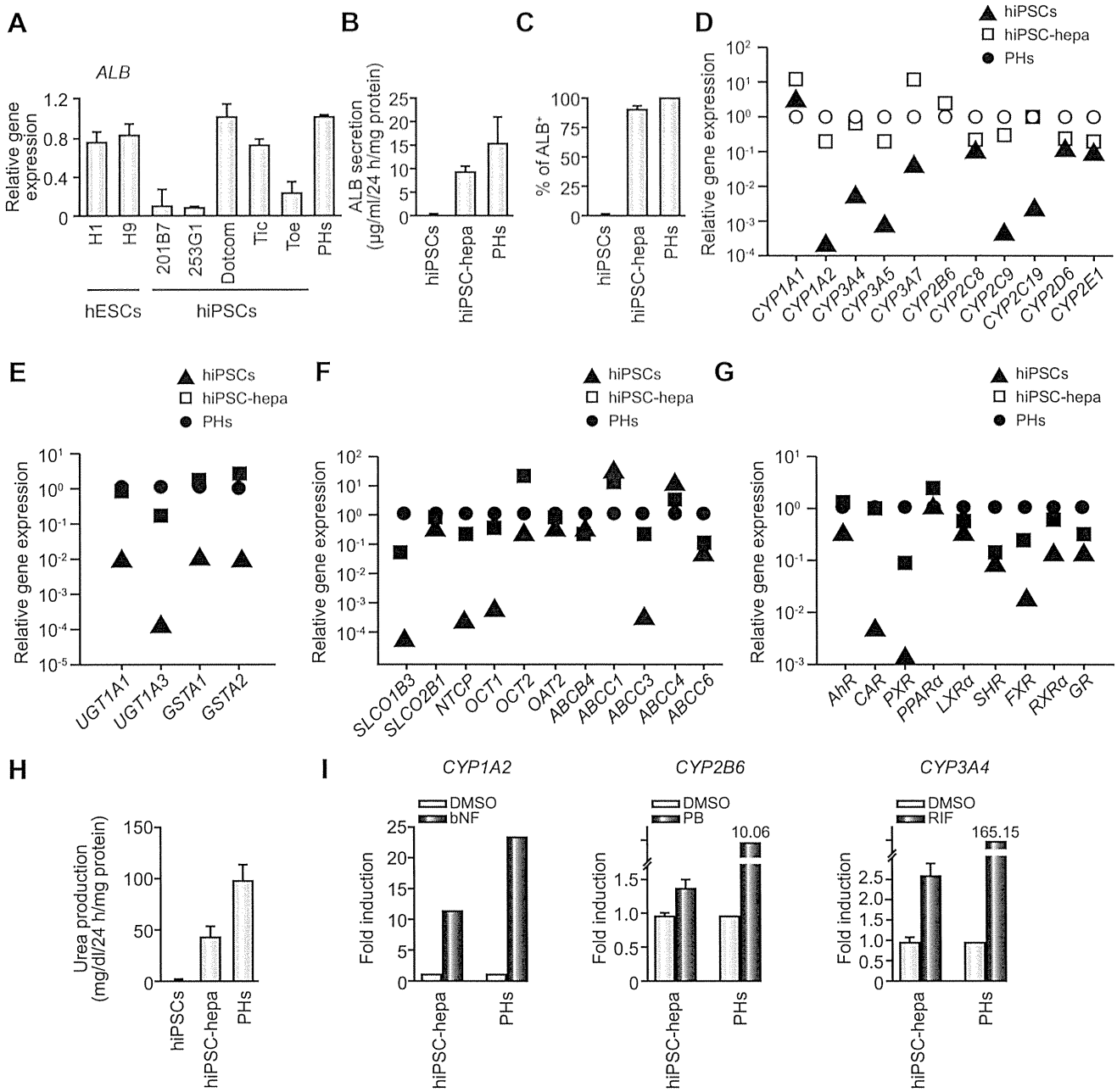

Fig. 3. The hepatic characterization of hiPSC-hepa. hESCs (H1 and H9) and hiPSCs (201B7, 253G1, Dotcom, Tic, and Toe) were differentiated into hepatocyte-like cells as described in Fig. 2A. (A) On day 20, the gene expression level of *ALB* was examined by real-time RT-PCR. On the *y* axis, the gene expression level of *ALB* in PHs, which were cultured for 48 h after cells were plated, was taken as 1.0. (B–I) hiPSCs (Dotcom) were differentiated into hepatocyte-like cells as described in Fig. 2A. (B) The amount of ALB secretion was examined by ELISA in hiPSCs, hiPSC-hepa, and PHs. (C) hiPSCs, hiPSC-hepa, and PHs were subjected to immunostaining with anti-ALB antibodies, and then the percentage of ALB-positive cells was examined by flow cytometry. (D–G) The gene expression levels of CYP enzymes (D), conjugating enzymes (E), hepatic transporters (F), and hepatic nuclear receptors (G) were examined by real-time RT-PCR in hiPSCs, hiPSC-hepa, and PHs. On the *y* axis, the expression level of PHs is indicated. (H) The amount of urea secretion was examined in hiPSCs, hiPSC-hepa, and PHs. (I) Induction of *CYP1A2*, *2B6*, or *3A4* by DMSO or inducer (bNF, PB, or RIF) of hiPSC-hepa and PHs, cultured for 48 h after the cells were plated, was examined. On the y axis, the gene expression levels of *CYP1A2*, *2B6*, or *3A4* in DMSO-treated cells, which were cultured for 48 h, were taken as 1.0. All data are represented as mean ± SD (n = 3).

dinately works to induce hepatocyte functions. Taken together, efficient hepatic differentiation could be promoted by using the combination of FOXA2 and HNF1α transduction at the optimal stage of differentiation (Fig. 2A). At the stage of hepatic expansion and maturation, Ad-HNF4α can be substituted for Ad-HNF1α (Fig. 1J). Interestingly, cell growth was delayed by FOXA2 and HNF4α transduction (Supplementary Fig. 5). This delay in cell proliferation might be due to promoted maturation by FOXA2 and HNF1α transduction. As the hepatic differentiation proceeds, the morphology of hESCs gradually changed into a typical hepatocyte morphology, with distinct round nuclei and a polygonal shape (Fig. 2B), and the expression levels of hepatic markers